LUND UNIVERSITY

Nano-Bio Interactions: The Myeloperoxidase Enzyme and Gallium Arsenide Nanowires

Cesare Mellace

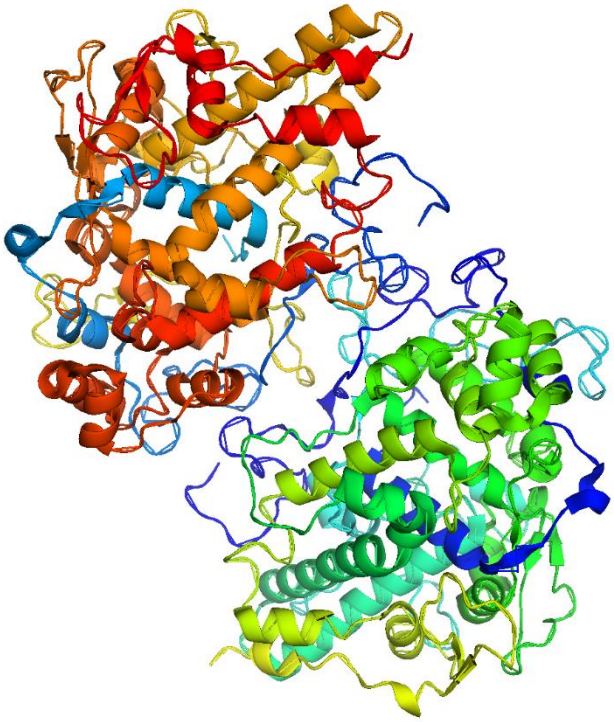

Thesis submitted for the degree of Master of Science
Duration of the project: 10 months

Supervisors:
Anders Mikkelsen, Tommy Cedervall
Faculty opponent:
Mathieu Gisselbrecht

Dedicated to My Parents

Disclaimer

The outcome of this work will be object of future publications.

Acknowledgements

First of all, I would like to express my gratitude to my family. Without their support, I would not have been able to complete this thesis or any other project I have ever taken up. Siete fantastici.

I am indebted to my supervisor, Tommy Cedervall, for the opportunity to work under his guidance which has been unfailing throughout this entire process. Jag ska inte glömma dina tipsar.

I appreciated the logistical help given by Anders Mikkelsen who permitted the birth of this jointed project between the department of synchrotron radiation physics and the department of biocìchemistry and structural biology.

I would like to acknowledge Stefan Gunnarson and Anna Carnerup of nCHREM for their invaluable assistance with the technical and practical aspects of this project.

An honorable mention goes to all of the colleagues who shared the office with me: Ida Lassen, Eglė Kelpšienė, Oskar and Eduardo Pèrez. All of them have been supportive and have promoted scientific discussion. Keep the great atmosphere we have built alive; do not let it fade away.

A special thanks to Hugo Öhrnemann for his fundamental help with the revision of some of the chapters included in this work.

Well-deserved recognition is given to Farai Chikwanha for making this thesis look better, in written English. Thank you for being the most important person I have met during my Swedish experience and for being here while I am writing these lines.

List of Abbreviations

ANS	1,8-Anilinoaphtalene
CRYO-EM	Cryogenic Electron Microscopy
DMA	Differential Mobility analyzer
FCAT	Fluorescence Correlation Analysis Tool
GaAs	Gallium Arsenide
GDP	Gross Domestic Product
HOMO	Highest Occupied Molecular Orbital
LM	Levemberg-Maquardt Method
LUMO	Lowest Unoccupied Molecular Orbital
MO	Molecular Orbital
MOVPE	MetallOrganic Vapor Phase Epitaxy
MPO	Human Myeloperoxidase Enzyme
NWs	Nanowires
PBS	Phosphate Buffered Saline
PFAST	Protein Fluorescence and Structure Toolkit
SCAT	Structure Correlation analysis Tool
TMB	3,3',5,5'-Tetramethylbenzidine
TRP	Tryptophan
VLS	Vapor Liquid Solid
XPS	X-Ray Photoelectron Spectroscopy

Table of Contents

List of figures

List of Tables

Introduction

The promise of a better future, of technological, human and environmentally-friendly progress has been recently associated with words like “nanotechnology”, “nanoscience”, and “nanomedicine”. It is almost as if the prefix “nano”, which means a millionth part of something, embodies the possibility for new and astonishing discoveries and capabilities. This is partially true. In fact, at the nanoscale, physical and chemical rules change, opening up fascinating solutions ranging from targeted drug delivery systems or highly efficient solar cells. Nonetheless, despite its positive possibilities, the nanoworld may potentially hide unexpected threats, which we have only just begun to understand. Viewing the nanoworld only as a boon for our development is like ignoring the dark side of the moon, and proceeding blind to anything other than the light of its benefits.

The likelihood that fragments of nanomaterials will come into contact with our bodies is not remote. Unregulated exposure to these entities is potentially a high-risk factor for the health of both operators in nanotechnology and the general population. Given this fact, nanotoxicology assessments have pivotal importance in the prevention of possibly dangerous outcomes deriving from the implementation of nanostructured materials in everyday devices. Therefore, this work aims at providing a deep, thorough analysis of both structure and functionality of Myeloperoxidase enzyme on Gallium Arsenide nanowires, nanometric designed materials usually implemented in solar cells as light harvesting enhancers.

The enzyme plays a major role in the processes of immune response in neutrophils leukocytes but also it is primarily involved in the development of autoimmune and cardiovascular diseases such as multiple sclerosis, and myocardial infarction. Understanding at a molecular level the interaction between the protein and the wires is, indeed, a pivotal step towards the evaluation of the toxicity profile for the Gallium Arsenide nanowires.

This work’s approach will be intrinsically multidisciplinary since, at the nanoscale, no tangible limit exists between physics and chemistry that are continuously interlaced. In my opinion, a non-sectorial method is needed to achieve satisfactory results and expand, the only present threshold in nanoscience which is the level of knowledge

In Chapter 1 a brief historical perspective on Myeloperoxidase discovery will be provided as well as the main structural features and catalytic pathway.

The synthesis and growth of Gallium Arsenide Nanowires from Aerotaxy will be treated in Chapter 2 that will also contain insights on the technical equipment required to perform the growth.

In Chapter 3 a of the experimental techniques used in this work will be started with the determination of the activity levels of Myeloperoxidase through standard absorbance enzymatic assay.

Chapter 4 is dedicated to a disquisition on luminescence phenomena with a focus on fluorescence and its role in protein spectroscopy. Different approaches to protein fluorescence will be investigated such as use of external dye molecules or exploitation of intrinsic fluorescence of aminoacidic residues. In the second section of the chapter there will be discussed the results of the different fluorescence experiments as well as the following computational analysis.

Chapter 5 will and unveil the potentialities of Cryogenic Transmission Electron Microscopy in the imaging of biomolecules at a relevant resolution. The chapter includes the images collected and a brief discussion on the conformational information that can be deduced.

In the end the conclusions section summarizes the findings and the future prospects relative to MPO analysis and the possibilities of investigation of bio/nano interactions via spectroscopy and microscopy techniques.

Chapter 1: Structure and functions of the green Enzyme Myeloperoxidase

1.1 Myeloperoxidase: a Swedish discovery

1941: the world is experiencing the apex of the Axis powers' expansion, the launch of the Barbarossa operation with the invasion of the Russian territory by the Wehrmacht puts the global equilibrium at serious threat [1]. Nonetheless Sweden, which at that time held a profile of belligerent neutrality i.e. formally not participating in the conflict but actually intensively trading with the Nazis Germany, was experiencing an increase in the Gross Domestic Product (GDP) that put the basis for the successive economic expansion in the post bellum period [2]. Under the bubble of neutrality Swedish scientific research funds could be addressed to non-military-oriented fields. These and many other reasons lie at the root of an important discovery made in the laboratories of the Karolinska institute where a medicine researcher Kjell Agner managed to extract a green glowing fluid from leukocytes in tuberculotic patients. From that fluid, Agner purified a previously unknown protein which named verdoperoxidase from the Latin word *viridis*, "green" and peroxidase due to the character of its enzymatic activity.

The same enzyme was subsequently extracted from bovines and appeared brown therefore the name was converted in Myeloperoxidase (MPO). With the improvement of crystallographic and protein crystallization techniques it was possible to reveal the structural featured and particularities of MPO that makes this enzyme unique within the same family of Peroxidases enzymes. These particularities as well as the reactivity of the green enzyme will be intensively discussed and analyzed in the subsequent sections of the chapter.

1.2 Myeloperoxidase: structure and general properties

Human Myeloperoxidase whose structure is depicted in figure 1 is a 148 kDa enzyme composed by two heterodimers symmetrically linked to each other via disulfide bonds and two Heme groups. The Heme group is a functional group present in multiple hematic proteins such as Hemoglobin, that enables the use of iron atoms . It is composed by four interconnected heterocyclic pentagons with Nitrogen atoms pointing towards the interior of the structure. In the center of the Heme is located an iron atom which is responsible for the functional role of the group [3].

Each dimer is formed by two different subunits: one heavier (58.5 kDa) and one lighter (14,5 kDa) for a total of 1140 amino acids[3]. The subunits are connected also via disulfide and heme linkages giving an overall C2 symmetry class to the protein, therefore MPO is invariant to 180

degrees rotation along its only symmetry axis [3]. The dimerization present in the three-dimensional structure is a peculiar trait of myeloperoxidase in comparison to the other proteins of the mammalian peroxidase family such as Lactoperoxidase (LPO), tyrosine peroxidase (TPO) which are composed only by one functional monomer [4]. The effect of this dimerization is still under investigation but the presence of two subunits does not seem to affect the functionality and activity rate of the enzyme but rather its thermal stability [4,5]. An underlying motivation for MPO's structure could be explained in an evolutionary attempt to strengthen the immune defense. In fact, pro-MPO i.e. the half-dimer, has similar activity compared to the fully dimerized form, but its thermal denaturation point is sensibly lower. [5]

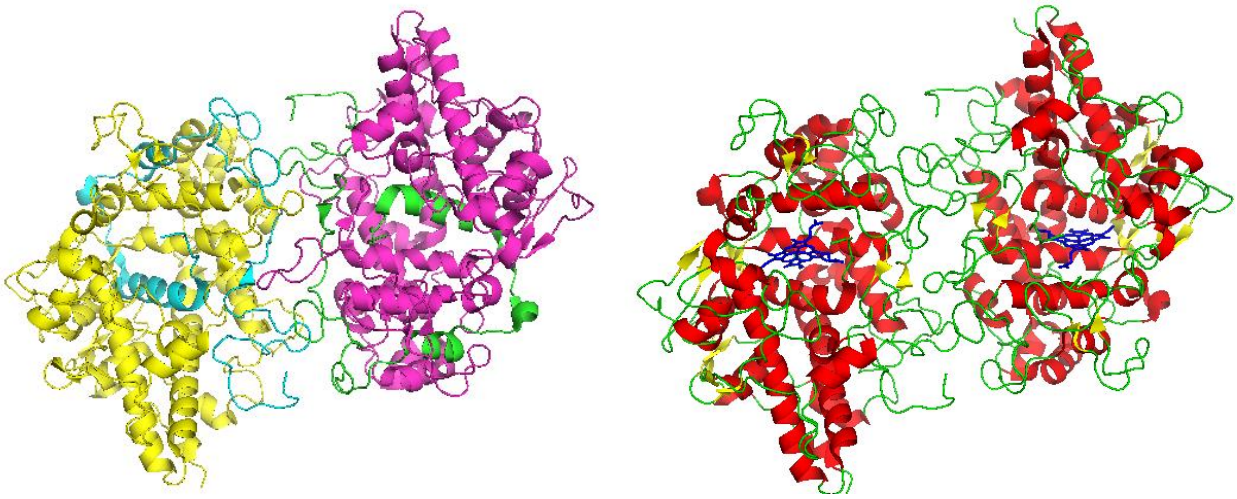

Figure 1 Crystallographic structure of the Human Myeloperoxidase enzyme. Left: colour coding relative to different chains and subunits. Right: colour coding according to secondary structure i.e. Loop in green, alfa helices in red, beta sheets in yellow Heme active sites in blue. Both structures were drawn with PyMOl v. from the 1CXP entry in the Protein Data Bank database

The secondary structure is primarily alpha-helical the core of which is comprised of five helices in the heavy subunit and one in the lighter subunit all linked to the active site of the heme. The complex architecture of Human myeloperoxidase´s active site has been revealed in 2000 with nearly atomic resolution (1.8 Å) by the crystallographic studies conducted by Tristan J. Fiedler et al.[6] The study highlighted the particular conformation of the Heme group which is not lying flat on the horizontal axis of the protein (see fig) but assumes a curved conformation through the linkage to histidine 95 and arginine 233 [6]. This unique disposition together with the aforementioned bonds is believed to be the cause of the exceptional MPO´s chlorinating activity with respect to other mammalian peroxidases. In fact. MPO's kinetic constant for the chlorination reaction is $2.5 \cdot 10^4\ M^{-1}s^{-1}$, in comparison to the kinetic constant of Lactoperoxidase (LPO), which is practically zero [3]. The kinetic constant measures the rates of variation of the velocity of the reaction,

The enzymatic reactions present in the following section dedicated to MPO's activity will be evaluated according to the kinetic constants considering the physiological condition and the

bioavailability in the leucocytes' phagososome i.e the leucocytes' organelle where bacteria are ingested and eliminated.

1.3 Reactivity and Physiochemistry

Myeloperoxidase is packed in the phagosome of neutrophils leucocytes whose represent the 5% of their dry mass. Neutrophils' are one of the first line of defence against bacteria like B.Anthracis or E.Coli [7,8]. Biochemically, the main task of peroxidases is unleashing the oxidative power of hydrogen peroxide to produce bactericidal compounds.

Consequently, the enzyme utilizes the peroxide as a substrate i.e as a cj to produce hypochlorous acid and chlorinated proteins which kill bacteria ingested by neutrophils leukocytes, as a first line defense against foreign bodies [3]. Figure 2 depicts the ensemble of reaction which characterizes MPO's catalytic profile

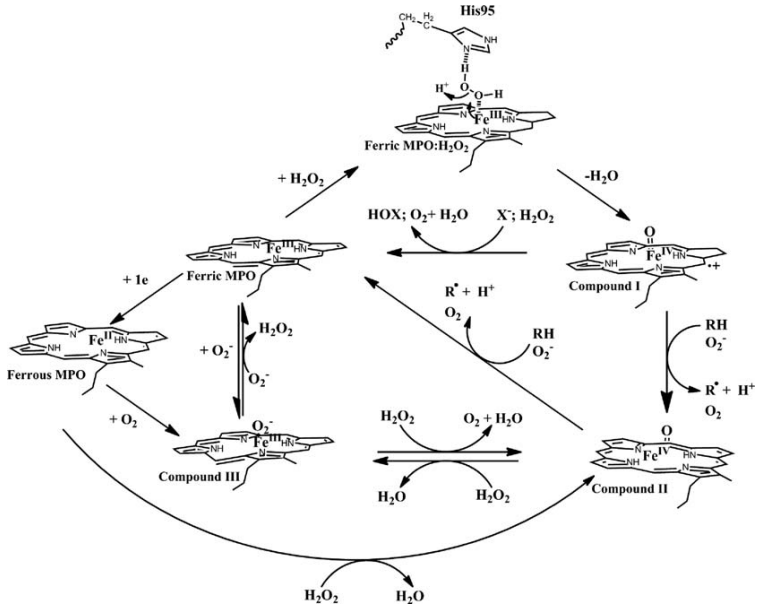

Figure 2 MPO's enzymatic profile: X represent halogen site mainly Cl^- but also Br^- or SCN^- while R is typically a protein residue like tryptophan and cysteine. Taken from [3]

MPO's cycle can be split in two subcycles: the halogenation cycle shown in figure 2 and 3 which actively produces the reactive oxidants deputed to bacterial killing and the dismutation cycle (left part of figure 2) that is necessary to manipulate the charge on the iron atom in the heme groups and regulate the overall enzymatic activity [3]. This complex mechanism involves the formation of 3 different reaction intermediates namely compound I, II and III which are differentiated by the oxidation number of the Iron atoms in the Heme pockets.

As depicted in the top area of figure 2 , the halogenation cycle is started by the H_2O_2 linkage to the ferric cation in the active site that is favored by the presence around the heme complex of two amino acids residues (His95 and Arg239) which are capable of hydrogen bonding towards the substrate with their nitrogen atoms. Once the peroxide is bound to the amino acid Histidine95 (His95), the enzyme catalyzes the heterolytic cleavage of the O-O bond via

transfer of a proton (H^+) from the oxygen bound to the iron atom to the other. The result is the formation of a water molecule that is liberated as a byproduct and an oxoferryl linkage (Fe=O-Heme) with the oxygen possessing six valence electrons which constitutes a strong oxidative site [3]. Compound I is deputed to the oxidation of halides through a bielectronic process that convert the anionic radicals (X^-) into hypohalous acids (HOX) after hydrolysis. The major substrates for this oxidation are chloride, bromide, iodide, and pseudohalide thiocyanate (SCN^-) which convert the enzyme back to its pristine ferric state.

The rate constants and the semi reaction are listed in table 1 that highlights the preferential oxidation for chlorine and slightly lower affinity for thiocyanate and bromine which can be inferred by the value of the relative reactive rate shown in table 1 [8]. While halides and thiocyanate oxidations have been proved to play a role in MPO biocatalytic activity, iodide reaction instead has limited physiological implications due to the insufficient concentration of the ion in physiological conditions [3]. This much appears from the value of relative reactive rate, which is at least one order of magnitude inferior to the others and can be physically explained by the superior dimension of the Van der Waals radius of iodide ion with respect to the others [3,8]. This superior dimension of iodine ion impedes an optimal configuration in the binding process to the Heme Group which in virtue of its particular conformation constitutes an highly-selective active site [3].

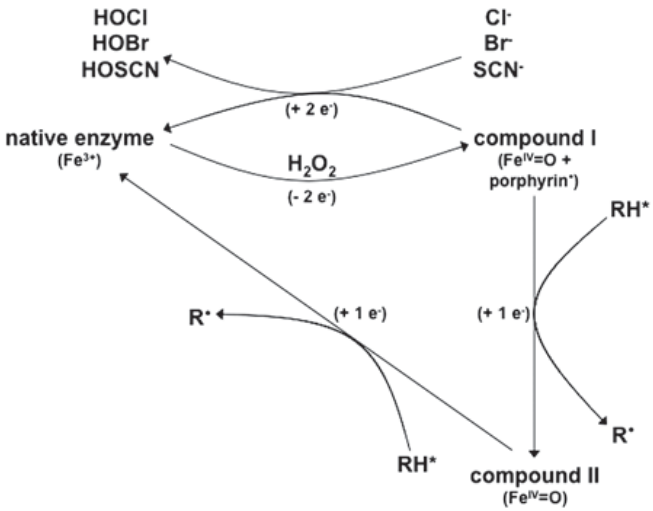

Figure 3 Detail on MPO's halogenation cycle. Taken from [8]

The high oxidative power of Compound I allows MPO to interact with even more substrates via monoelectronic routes that transform the enzyme in compound II, an oxoferryl complex but with sensible lower reactivity. The intermediate Compound II requires an additional oxidation step in order to regenerate the active ferric Myeloperoxidase and close the peroxidase cycle [8]. The typical substrates for compound II are amino acids like tryptophan and cysteine which suggest an active participation from MPO in the halogenation of proteins which causes dysfunctional behavior that can lead to ultimately the death of the organism affected [8].

The nitric ion is important to the biological consequences because it is only oxidized via one electron process by compound I. This oxidation leads to the generation of peroxynitrous acid

($ONOO^-$), a highly reactive specie that is responsible for nitrosation of tyrosine residues in proteins [3]. The biological implications of MPO´s reactive product can be retrieved here [4-5].

Table 1 Rate and affinity parameters for compound 1 bielectronic substrates. The value of the relative reactive rate evidences the preferential substrates for the conversion of Ferric MPO into Compound I. Modified and adapted from [3]

Substrate	Chloride	Bromide	Iodide	Thiocyanate	Hydrogen peroxide
Half-reaction	$HOCl/Cl^-$ ($Cl_2/2Cl\_$)	$HOBr/Br^-$ ($Br_2/2Br\_$)	HOI/I^- ($I_2/2I$)	$HOSCN/SCN^-$ ($(SCN)_2/2SCN\_$)	O_2/H_2O_2
[Substrate] (mM)	100	0.02–0.1	<0.001	0.02–0.2	<0.01
Reactive rate (k)	$2.5 \cdot 10^4$	$1.1 \cdot 10^6$	$7.2 \cdot 10^4$	$9.6 \cdot 10^4$	$2.2 \cdot 10^6$
Relative reactive constant $k \cdot [substrate]$	2500	20–100	<7	200–2000	< 20
Van der Waals Radius	1.81 [9]	1.96 [9]	2.02 [9]	1.86 [10]	n/a

As previously mentioned, labelling MPO as a pure peroxidase enzyme is quite reductive with respect to the actual catalytic profile of the enzyme that also exhibits considerable superoxide dismutase activity. The enzyme catalyzes the production of the superoxide radicalic anion O_2^- via reversible dismutation of hydrogen peroxide [3]. The secondary dismutation pathway is started by the reduction ferric enzyme to ferrous MPO by radicalic anions formed in the one electron oxidation of compound II e.g. hydrogen sulphide serotonin and melatonin [8]. Ferrous MPO is oxidized by molecular oxygen to form compound III whose peculiarity consist in the superoxide ion bound into the heme pocket. Compound III is converted reversibly into the Ferric enzyme by release of the superoxide complex, the released ions are, in physiological condition, oxidized to H_2O_2 to restore the initial condition for the halogenation cycle [3].

Nonetheless, in the bacterial killing process, oxygen concentration in leucocyte's phagosome where MPO is stored drops considerably due to the leuckocyte respiratory burst. In this hypoxic environment there is a remarkable probability that the dismutation of superoxide anion leads to production of singlet oxygen. The lowest excited molecular state of oxygen ^1O is far more reactive than its triplet counterpart and it is identified as a marker for oxidative stress scenarios which directly causes genetic damage to bacteria [11].

As shown in this chapter, the majority of the products and reactions of myeloperoxidase involve oxido/reductions and produce highly reactive substances e.g. which are primarily intended to preserve human organisms from foreign aggression. Those compounds, though, are even more dangerous for the human tissues in case they are ejected outside the phagosome, MPO oxidants are believed to play a fundamental part in the development of numerous and different diseases from Coronary artery disease to Multiple Sclerosis [12]. The consequences of an anomalous behaviour of the green enzyme as well as its biosynthetic assembly are left to the reader [13-14].

References

[1] Christer Bergström, *Barbarossa - The Air Battle: July-December 1941*, Londra, Chervron/Ian Allen, 2007, ISBN 978-1-85780-270-2.

[2] Golson, Eric *The economics of neutrality : Spain, Sweden and Switzerland in the Second World War London School of Economics and Political Science,* University of London, 2011 http://ethos.bl.uk/OrderDetails.do?uin=uk.bl.ethos.547243

[3] A.J. Kettle, C. C. Winterbourn, *Myeloperoxidase: Structure and Function of the Green Heme Peroxidase of Neutrophils,* Chapter 12 in *Heme peroxidase edited by Emma Raven, Brian Dunford* RSC 2015 ISBN 978-1-78262-262-8

[4] I. Grishkovskaya et al. *Structure of human promyeloperoxidase (proMPO) and the role of the propeptide in processing and maturation* 2017, Jour. Bio. Chem. 292 (20) : 8122 – 8543, DOI 10.1074/jbc.M117.775031 X

[5] Hansson, M., Olsson, I., & Nauseef, W. M. (2006). Biosynthesis, processing, and sorting of human myeloperoxidase. Archives of Biochemistry and Biophysics, 445(2), 214–224. https://doi.org/10.1016/j.abb.2005.08.009

[6] Tristan J. Fiedler, Curt A. Davey and Roger E. Fenna X-*ray Crystal Structure and Characterization of Halide-binding Sites of HumanMyeloperoxidase at 1.8 Å Resolution* J. Biol. Chem. 2000, 275:11964-11971. doi: 10.1074/jbc.275.16.11964

[7] V. Brinkmann -"*Neutrophil engulfing Bacillus anthracis*". PLoS Pathogens 1 2005 (3)

[8] David I. Pattison, Michael J. Davies & Clare L. Hawkins (2012) Reactions and reactivity of myeloperoxidase-derived oxidants: Differential biological effects of hypochlorous and hypothiocyanous acids, Free Radical Research, 46:8, 975-995, DOI: 10.3109/10715762.2012.667566

[9] Van der Waals Radii of Elements S. S. Batsanov Inorganic Materials, Vol. 37, No. 9, 2001, pp. 871–88

[10] Y. Iwadate, K. Kawamura, K. Igarashi, and J. Mochinaga, *Effective ionic radii of nitrite and thiocyanate estimated in terms of the Boettcher equation and the Lorentz-Lorenz equation,* J. Phys. Chem., 1982, 86 (26), pp 5205–5208 DOI: 10.1021/j100223a028

[11] F.Arisawa,et al. *MCLA-dependent chemiluminescence suggests that singlet oxygen plays a pivotal role in myeloperoxidase-catalysed bactericidal action in neutrophil phagosomes* Lum 2003, 18 (3) https://doi.org/10.1002/bio.728

[12] S. J. Klebanoff *Myeloperoxidase: friend and foe*, 2005 Jour. Leuk. Bio 77 (5) https://doi.org/10.1189/jlb.1204697

Chapter 2: Gallium Arsenide Nanowires

"*There is plenty of room at the bottom*": the iconic phrase pronounced in 1959 by Richard Feynman is, nowadays, globally recognized as the birth of the idea of nanotechnology [1]. Manipulation at the nano or atomic scale was already predicted in his visionary speech, which in addition foresaw the extremely competitive environment of postmodern science. The spirit of challenge is well represented through the institution of a prize addressed to the solver of the Encyclopaedia Britannica's challenge. "Why cannot we write the entire twenty-four volumes of the entire Encyclopaedia Britannica on the head of a pin?" these are the words used by the famous scientist to throw the gauntlet in the completion of what he pointed as a milestone in the development of nanotechnology [1]. What does it actually mean to fulfil Feynman's challenge? What are the dimensions involved in the completion of the challenge? As Feynman speech progresses, he claims that to win the challenge it is necessary to develop a technology to write 25000 times smaller than usual and 25000 times smaller than the resolution limit of the human eye [1]. Feynman's prize was unclaimed until 1985 when Tom managed through lithography to imprint the first two pages of the Encyclopedia Britannica on the head of a pin.

What if instead of considering only the head of the pin we considered the shaft of the pin?

The common dimension for the length of pin shafts is in the order of centimetres, if we demagnify it by the same 25000x factor we obtain few hundredths of nanometers which correspond to the characteristic length of an another important nanomaterial: Nanowires. Nanowires are usually semiconductor materials whose length ranges from hundreds of nanometers to several micrometers. Their longitudinal dimension greatly overcomes their diameter which is typically limited between few and tens of nanometer.

In this chapter the point of focus will be brought on one of the many techniques to produce this typology of nanomaterial i.e. Aerotaxy. The aerotaxy method has been proven to reduce considerably the costs for the production of nanowires, making it a feasible candidate for device prototyping for the advent of a new generation of solar cells [2]. Recently, the whole technique has been patented and Sol Voltaics is already launching the commercialization of novel solar cells based on this nanostructure. Therefore, the likelihood that nanowires produced via aerotaxy will come into contact with the human body must not be underestimated. This chapter, though, will be dedicated to the principles of nanowires growth.

2.1 Nanowires Vapor Liquid Solid Crystal growth

Semiconductor materials base their electronic and optical properties on their crystalline structure and orientation. Therefore, the growth mechanism and orientational control play fundamental roles in ruling the overall applicability of the grown material. The most prominent approach to the growth of nanowires material is called VLS method, i.e. Vapor-Liquid-Solid, which consist of the formation of a triphasic system at the eutectic composition. This system acts as a nucleation center that favors the generation of wired crystals [3]. The vapor phase is composed by the gaseous precursors for the growth, in the case of Gallium Arsenide nanowires the precursor are Trimethyl Gallium and Arsenic hydride that react as depicted below [4]

$$(CH_3)_3Ga + AsH_3 \longrightarrow GaAs + 3\,CH_4$$

The liquid phase is constituted by a gold droplet acting as a catalyst for the formation of an eutectic alloy that seeds nucleation and growth of the wires. The solid phase are wire-shaped grown crystals. An overview of the process is shown in Picture 4 [5].

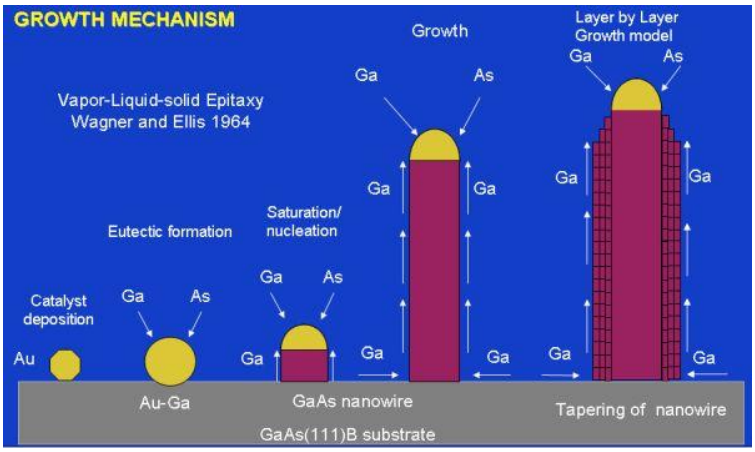

Figure 4 VLS epitaxial growth method with substrate assisted technique.From left: Deposition of Au catalytic droplets; particle-assisted eutectic alloy formation; injection of precursor causes supersaturation and nucleation of the solid phase epitaxtial growth of nanowires. Taken from [5]

Generally, the formation of a crystal phase is a manifestation of a more general principle called le Chatelier-Brown principle which establishes that a system evolves in order to minimize the effect of any perturbation induced. Therefore, to counteract the effect of the injection of new material the system tends to form a solid phase to bring back system to the concentration of equilibrium [3].

VLS growth principle relies on the perturbation of the thermodynamic equilibrium when the gaseous precursors are injected in a reactor. Quantitatively the possibility of crystal growth can be computed thermodynamically via the Gibbs free energy function which takes in account all the contributions to the equilibrium state of the system, mainly, concentration of species, pressure and temperature. The equilibrium condition is set with:

$$dG_{a,b} = 0$$

Where a and b are the physiochemical variables of interest that are kept constant. In the case of nanowires, the crystal growth is triggered by the introduction of the gaseous precursors so through a variation of the concentration of chemical species in the system. This modification is taken in account with the concept of chemical potential that is defined as the rate of variation of gibbs free energy function with respect to the moles of the i-th substance in the system at constant temperature and pressure [6] .

$$\mu_i = \left(\frac{dG}{dN_i}\right)_{T,P} [6]$$

With chemical μ_i potential of the i-th component, G is the Gibbs Free Energy, N is the number of moles of the i-th chemical specie. Thus, a variation in the chemical potential perturbs the thermodynamic equilibrium initiating the growth process. Since the volume of the reactor is constant the change in chemical potential can be expressed in terms of concentrations

$$C = \frac{N_i}{V}$$

if V is constant C proportional to Ni

$$dG = d\mu_i = kTln\left(\frac{C_{1,i}}{C_{eq,i}}\right)_{T,P} [6]$$

Whenever the $c_{1,i}$ so the concentration of the growth species is superior to the equilibrium concentration, the system is in a condition of supersaturation. So, the excess in free Gibss energy (dG>0) constitutes the driving force for the formation and development of a solid phase that brings back the system in the equilibrium condition.

2.2 VLS techniques: Aerotaxy

The VLS growth method used for the production of the NWs used in this thesis is called aerosol-epitaxy, commercially known as Aerotaxy. This method is an innovative production technique recently developed in Nanolund's laboratory designed to provide a platform for a large-scale production of nanowires with high quality standards. Its first concept was suggested by Deppert et al [7] who firstly proposed a combination between aerosol catalysis and epitaxial growth to achieve self-assembled nanocrystals. Aerotaxy permits the complete removal of the monocrystalline catalytic surface present in standard Metallorganic vapor phase epitaxy (MOVPE) reactors. In the Aerotaxy reactor, the nucleation and epitaxy processes occur on the surface of aerosolized gold particles in comparison to the surface of a monocrystalline substrate as usual in MOVPE (fig 5) [4]. The removal of the catalytic surface allows to increase the throughput about 50 times since there is no spacial limitation for the number of gold particles that are placeable per unit of semiconductor surface. The typical growth rate is in the order of

the micrometer per second which results in a production of approximately 10^{11} nanowires per hour [4].

This enhanced efficiency put the basis for the industrial development and inclusion of the aerotaxy technique as a method for the construction of light harvesting layers in high quality solar cells. A schematic of the aerotaxy reactor present in Nanolund labs is shown in the picture below:

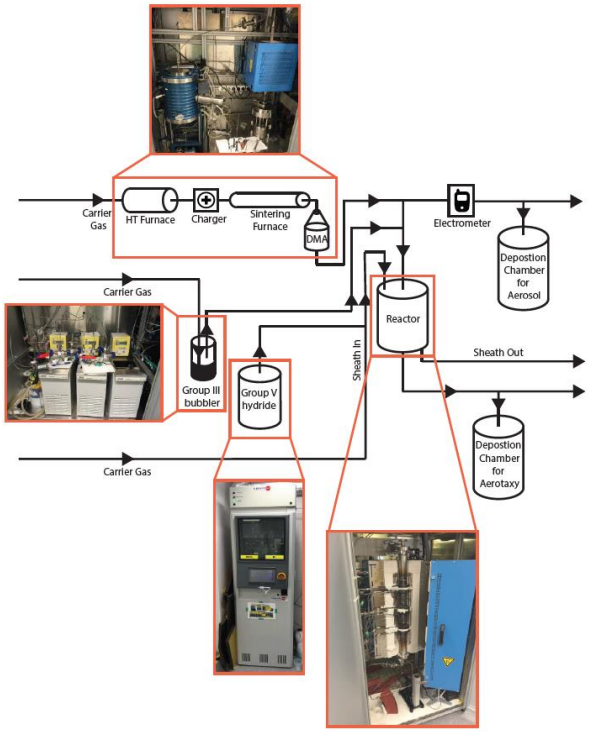

Figure 5 Aerotaxy reactor In NanoLund [8]

The process starts with the generation of Au Nanoparticles in a hot furnace (HF) at 1400-1500 °C subsequently the particles are charged to allow filtering via Differential Mobility Analyser (DMA) in order to obtain a narrow distribution of nanowires diameters [8]. The differential mobility DMA is composed by two opposite charged plates which discriminate particles according to their charge to mass ratio since the flow trajectory is affected by the electric force of the analyser. Further details on the DMA can be found here [2]. Once the desired catalyst has been produced the gaseous precursors, transported in ultrapure nitrogen as a carrier gas, are injected into the reactor previous passage in a mass-flow control system that ensure a constant flux of the chemical species [8]. This flux is kept in laminar flow regime to avoid any uneven distribution of concentration in different areas of the reactor that would affect the growth process of the wires. Nevertheless, there is some variability in the length of wires collected due to the parabolic flow profile caused by the effect of the walls of the reactor [4,8]. The collection of the wires happens on a silicon surface only successively dispersed in ethanol to prevent oxidation of surface and eventual desorption of potentially dangerous arsenide ions as shown by near ambient pressure XPS measurements [9].

REFERENCES

[1] Feynman, R.P., *There's plenty of room at the bottom*, Eng Sci, 23 (1960), pp. 22-36

[2] Heurlin, M., Lindgren, D., Deppert, K., Samuelson, L., Magnusson, M.H., Ek, M.L., Wallenberg, R., *Continuous gas-phase synthesis of nanowires with tunable properties*,(2012) Nature, 492 (7427), pp. 90-94.

[3] Persson, A., *Epitaxial Growth of semiconductor Nanowires*, Doctoral thesis, Department of physics, Solid State Physics division (2014), Lund university

[4] Heurlin, M., *Aerotaxy: A Gas phase Nanowire growth technique*, licentiate thesis, department of physics, solid state physics division (2014), Lund university

[5] D.L. Dheeraj, H.L. Zhou, A.F. Moses, T.B. Hoang, A.T.J. van Helvoort, B.O. Fimland and H. Weman. *Heterostructured III-V Nanowires with Mixed Crystal Phases Grown by Au-Assisted Molecular Beam Epitaxy*, 2010, Chapter 2 in *Nanowires*, book edited by Paola Prete ISBN 978-953-7619-79

[6] Heurlin, M., *Aerotaxy: Growth of Semiconductor Nanowires for Solar Cells Application*, Doctoral dissertation, Department of Physics, Solid state physics division (2015), Lund university ISBN 978-91-7623-506-5

[7] K. Deppert K., Bovin, J.-O., Malm, J.-O., Samuelson, *L. A new method to fabricate size-selected compound semiconductor nanocrystals: Aerotaxy (1996)*, Journal of Crystal Growth, *169 (1), pp. 13-19*

[8] Yang, F., *Growth and Regrowth of Nanowire Materials*, licentiate thesis, Department of Physics, Solid State Physics division (2015), Lund university

[9] Zhang, X., Lamere, E., Liu, X., Furdyna, J.K., Ptasinska, S.,*Interface chemistry of H2O on GaAs nanowires probed by near ambient pressure X-ray photoelectron spectroscopy*,(2014) Chem. Phys. Lett., 605–606, pp 51-55,

Chapter 3: Colorimetric enzymatic assay

Enzymes are the engines of life, the motors of a series of well-orchestrated chemical reactions. Without their action, the Earth would have a radically different look deprived of all the forms of life that populate the blue planet, including man. Enzymatic catalysis permits the modification of chemicals in time frames compatible with life.
Crucially essential, enzymes have been object of human interest since ancient times, when the first reports from different civilizations such as Egyptian or Babylonian suggested the utility of microorganisms in the fermentation of cheese and wine [1].
Time passed and the involvement of enzymes in human life has dramatically increased as well as the awareness of their functionalities. Nowadays, the impact of enzymes is not limited only to the food technology sector but also in multiple other e.g. chemical industry or pharmaceutical research. Protein stains would be difficult to remove without the contribution of proteolytic enzymes present in detergents, at the same time, designing of specific enzyme inhibitors is a valid strategy to cure diseases that are dependent on enzymatic anomalies [1].
The common denominator for the exploitation of these biomolecules is the awareness and detailed knowledge of their functional mechanism.
In this chapter the point of focus will be brought on one of the multiple techniques to study enzymatic behaviour i.e colorimetry

3.1 Activity and colorimetry

Colorimetric assaying is one of the most widely spread technique among of all the methods used to measure the endpoint value for enzymatic activity due to its simplicity, robust theory support, efficiency and discrete reliability. The basic principle of colorimetry is the attenuation of light going through a solution of different chemical species, this phenomenon was firstly investigated in 18^{th} century by Lambert [2].
Consider a flux of light travelling along the z axis that is intercepted by an infinitesimal slab of solution with a surface S and length dz. In this infinitesimal volume S*dz are present a quantity N of molecules approximated as not overlapping discs.
The variation of flux can be estimated as

$$\frac{d\phi}{dz} = \sigma N \phi \text{ [3]}$$

Where σ is the cross section relative to all possible interactive phenomena e.g scattering and luminescence.

The solution to this simple differential equation is

$$\phi_f = \phi_0 \, exp(-N\sigma z) \text{ [3]}$$

Therefore, the fraction of light transmitted i.e the transmittance is defined as follows

$$T = \frac{\phi_f}{\phi_0} = exp(-N\sigma z) \text{ [3]}$$

the definition of optical depth (τ) and absorbance (A) allow to linearize the equation

$$\tau = -ln\,(T);\; A = -\log_{10}(T)$$

$$A = \tau / ln10$$

$$A = -\left(\frac{1}{ln10}\right) \cdot (-N\sigma z)$$

Supposedly there is no scattering or luminescence phenomena occurring in the solution e.g fluorescence or phosphorescence, the cross section can be written in term of the attenuation coefficient epsilon following the equations below [4]

$$\epsilon = N_a \frac{\sigma}{ln10}$$

But

$$C = N/N_a$$

Thus,

$$A = \left(\frac{1}{ln10}\right) \cdot ln10 \cdot \epsilon C z = \epsilon C z$$

With z optical path i.e the length of the light travelling within the solution

In conclusion, the absorbance of a solution is linearly dependent on the concentration of chemicals within it. If the absorbance varies with the wavelength in the visible range the sample of interest will change colour since only selected wavelengths will be transmitted, which is the basic principle of colorimetry.
Thus, to colorimetric quantify the enzyme activity is necessary to correlate the variation of an enzymatic property with the activation of an optical absorbing substance i.e. a chromophore
The chromophore can be constituted by a dye compound or even by the enzyme itself.
For mammalian peroxidases and, in particular MPO, neither hydrogen peroxide or the proteins are optically active in the visible range, therefore, to perform a colorimetric assay an external chemical is needed. MPO's peroxidase reactions to form compound I and II belongs to the category of oxidoreductions that presume a net transfer of electrons from a compound to another.
In the colorimetric assay the electron transfer is used to trigger the excitation of a molecule of 3,3',5,5'-Tetramethylbenzidine (TMB) which upon oxidation converts the solution colour to blue with an absorption peak at 650 nm.
The pivotal reactions for the assay are listed below:

$$Porphirin\ Fe^{III} - 2e^{-} \longrightarrow (Fe^{IV} = O) + Porphirin^{+}$$

$$TMB + 2e^{-} \longrightarrow TMB^{*}$$

The limitations for such a colorimetric endpoint assay are strictly related to the fundamental restrictions of colorimetry itself.

Absorbance measurements deal with the intensity of the monochromatic light that is not absorbed by the sample. In order to detect low variations of chromogenic substrates small differences in transmitted intensity must be measured in a regime of considerably high light intensity. Moreover, the logarithmic relationship between optical absorbance and the intensity of transmitted light constrains the sensitivity at high chromogen concentrations because remarkable large variations in optical absorbance correspond to very small differences in the intensity of unabsorbed light [4]. Consequently, the range of validity for colorimetric assays readings should lie in the range 0.1 to 1.5 arbitrary units.

Given all these consideration colorimetry remains one of the most vastly used methodologies in routinely chemical analysis, in this thesis absorbance measurements were carried out to estimate the effect of the interaction between Gallium arsenide nanowires and Human Myeloperoxidase Enzyme.

3.2 Spectral absorbance and activity

The colorimetric assay chosen to evaluate MPO's activity in this thesis is a colorimetric assay using TMB as marker. TMB optical properties are well-known and characterized as well as its low toxicological profile which promotes the dye as the ideal candidate for oxidoreductase assays

In attempt to model the behaviour of enzyme in physiological environment the possibility of quenching the reaction in sulphuric acid with an assay on the absorbance peak at 400 nm has been neglected due to the fact that it is quite unlikely that the pH within the leucocytes' phagosome will drop abruptly [5].

The correct evaluation of GaAs NWs contribute to MPO's enzymatic behavior requires a subsequent series of experiments in order to benchmark and reference the assay because of the different cohexistence of multiple chemical species in the reaction mixture. At principle, though, the following colorimetric assay protocol was validated by testing at different concentrations of protein. All the absorbance measurements have been performed with the ProbeDrum spectrometer otherwise stated differently. Human MPO enzyme was purchased by abcam, PBS Dulbecco's phosphate buffer from Sigma Aldrich, Hydrogen peroxide 30% in H_2O stabilized and TMB easy substrate from Sigma. All the mixtures were prepared in Eppendorf tubes then transferred via pipetting procedure in 2000 µl Polystyrene Cuvette.

The standard assay solution consisted in

- 50 µl PBS buffer solution with MPO in dilution series
- 100 µl TMB easy substrate

- 1,02 µl/ml Hydrogen Peroxide in Sodium acetate buffer
- 100 µl Sodium acetate buffer

The dilution series was operated by adding different volumes of 100 µ/ml MPO solution starting from 10 µl up to 0 µl with step of 2 µl for each series of triplicates; the final concentration of protein in the sample is calculate. In total 18 cuvettes were prepared and tested over time of 4 hours, the storage of the samples was effectuated at room temperature. The plot below shows the variation of the absorbance spectra for the different enzymatic concentrations.

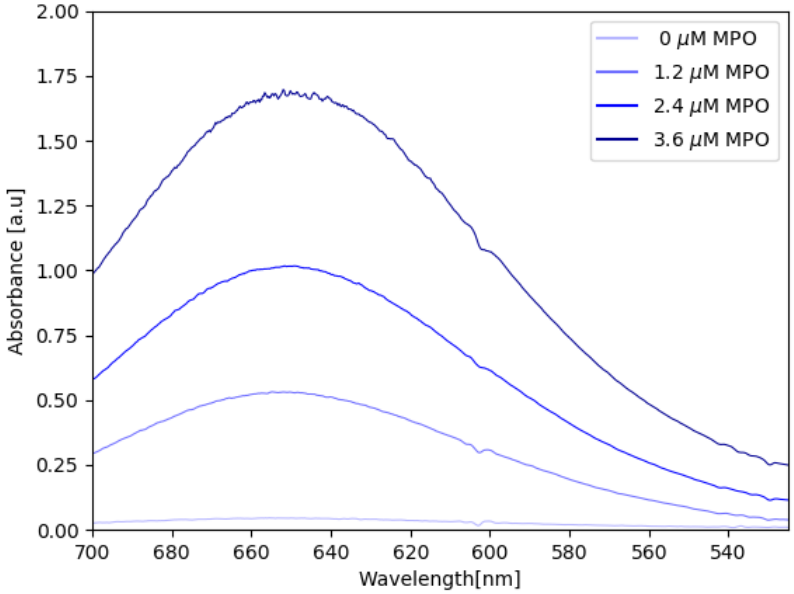

Figure 6 Myeloperoxidase absorbance variation with respect to volume of enzyme used. Spectra recorded at time t=90 min

Once all the spectra were collected a more robust analysis was carried out in order to retrieve the position of the maximum and the intensity for each sample. This endpoint value permits the calculation of the enzymatic activity so particular accuracy is necessary to obtain reliable values. Overall, the data treatment was performed with via Fityk version 0.9.8: an open source spectral analysis software [6]. Fityk v0.9.8 has embedded different peak fitting procedures, for the aforementioned dataset the fitting procedure utilized was the Levenberg-Marquard method (LM) [7]. A detailed description of the method goes beyond the goal of this thesis, but it can be retrieved here [7]. The LM method requires an initial guess of a function for the deconvolution, for the aforementioned dataset, the fitting function was chosen to be the log-normal function. The log-normal function provided the least residual error estimated as weighted sum of squared residuals (WSSR) i.e. the chi-square value, at the end of the fitting procedure [7].

Subsequent to the fitting procedure, it was possible to plot the variation of the absorbance peak over time and establish the optimal concentration as depicted in figure 7.

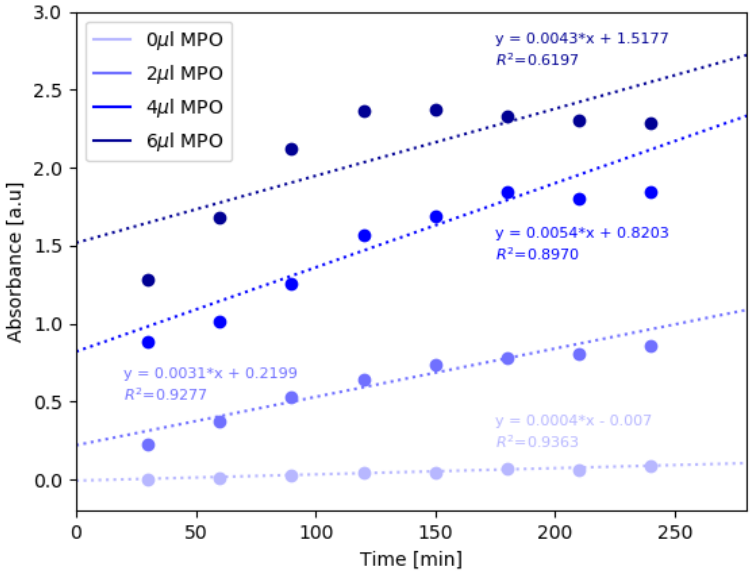

Figure 7 Myeloperoxidase validation assay.
The 3.6 µM data points are clearly not reliable for activity calculation due to saturation of the detector.

Considering that 1 mol of H2O2 produces 0.5 mol of the charge-transfer complex that absorbs at 650 nm the final endpoint value absorbance is proportional to the concentration of activated TMB in the mixture. Quantitatively, the enzymatic activity can be calculated as follows

$$a\left[\frac{U}{ml}\right] = \frac{\Delta A_{650\ \mathrm{nm}}}{min} \cdot\ 5.13\ [5]$$

Table 2 MPO's activity values. The 3.6 µM series is not shown due to insufficient reliability of the experimental data

MPO concentration [µM]	Activity [mU]
0	2.05
1.2	15.92
2.4	27.70

The interesting quality parameters for the validation of the assay is the linear fit of the data point in the time domain and the linearity with the respect to the enzymatic concentration. In figure 7 the degree of linearity between absorbance and time is expressed by the correlation factor R-squared that shows the level of linear interdependence of the two variables i.e. the goodness of the linear fit [7]. The R-squared factor is calculated as

$$R^2 = \frac{\sum(x - \bar{x})\,(y - \bar{y})}{\sqrt{\sum(x - \bar{x})^2 \sum(x - \bar{x})^2)}}\ [8]$$

Where $\bar{x}$, $\bar{y}$ are the average values of the dataset. R-squared value ranges from 0 to 1 and it can be easily interpreted as a percentage of resemblance of the data points with the line guessed.

Considering the data shown in figure 7, it is remarkably evident that the value of the correlation factor decreases after 4µl; this fact can be explained through the limited sensitivity of the experimental setup. The values of absorbance represent the quantity of light intercepted by the solution on a logarithmic scale therefore a variation of 1 point in absorbance means that the light collected at the detector is 10 times inferior than the incident. Considered the capabilities of the instrumental setup and the theoretical limitation explained in the previous section of the chapter, the high confidence range of the measurements is between 0.1 and 1.5 arbitrary units [4].

Therefore, the best value for MPO stock solution volume selected for the successive steps of the assay has been chosen to be 3 µl which corresponds to a concentration of 4.8. 10^{-5} mM.

3.3 MPO NWs assay

1 ml of Aerotaxy grown GaAs Nanowires produced by Martin Magnusson in NanoLund lab dispersed in ethanol have been stored in aliquots of 50 µl per Eppendorf's tube, at room temperature. Given the high velocity of sedimentation, which is easily detectable by the formation of a brown precipitate, the GaAs NWs were sonicated in a water batch for 30 seconds to recreate a homogeneous dispersion. Then 5µl of the dispersion were added to the optimal solution established as mentioned before, and the activity tested in the same fashion. Triplicates of the 3µl MPO solution without addition of NWs solution were tested as a positive control.

The assay mixture consists in:

- 42 µl PBS buffer solution of which 3 µl MPO + 5 µl GaAs NWs in ethanol / 5µl PBS in control
- 100 µl TMB easy substrate
- 1,02 µl/ml Hydrogen Peroxide in Sodium acetate buffer. Total volume 100 µl

The data analysis procedure was conducted as explained previously and led to the following results

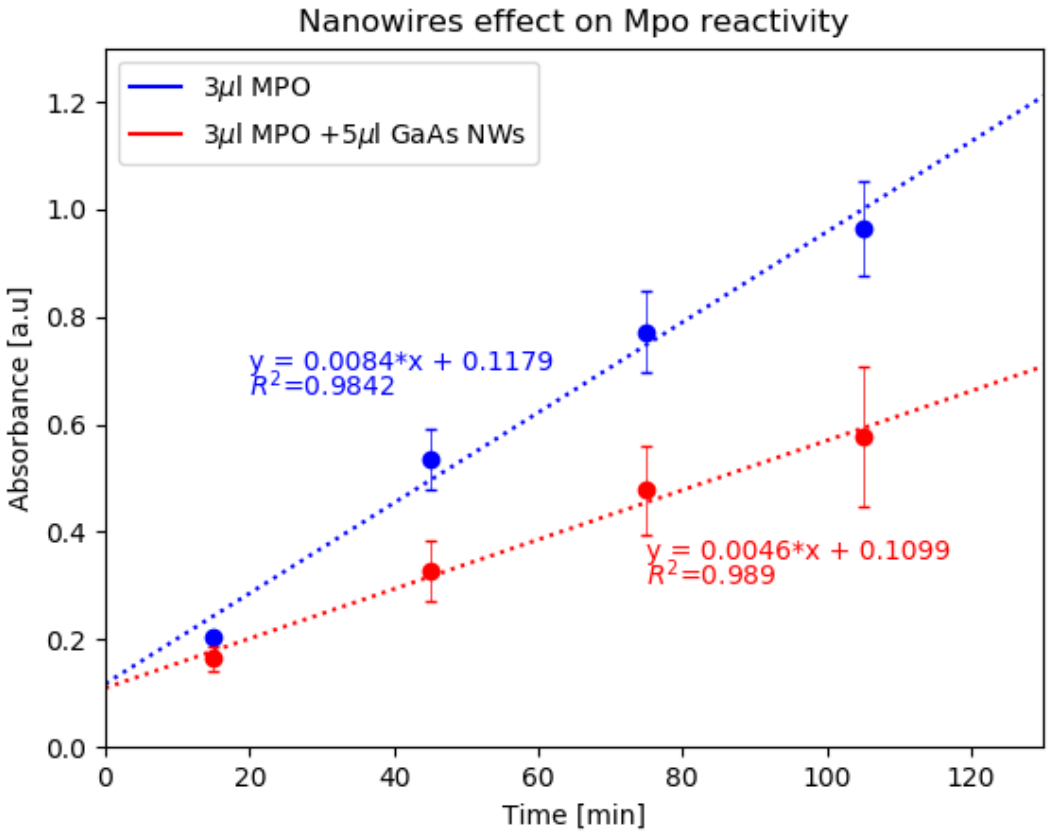

Figure 8 Gallium Arsenide Nanowires' effect on MPO enzymatic activity

From the data collected, a reduction in the steep of the model line is clear. This represents a reduction in the rate of absorbance. Quantitatively, according to previous equation, MPO's activity can be calculated as: [5]

$$a_{mpo} = 0.084 \cdot 5.13 \cdot 1000 \left(\frac{mU}{U}\right) = 43.26$$

$$a_{mponw} = 0.046 \cdot 5.13 \cdot 1000 \left(\frac{mU}{U}\right) = 23.59$$

$$\%\frac{a_{mponw}}{a_{mpo}} = \frac{23.59}{43{,}26} \cdot 100 = 54\%$$

The experimental data supports a remarkable reduction of the enzyme activity when the nanowires are added to the proteic solution which suggests an interaction between the nanomaterial and the biomolecule.

3.4 Binding Assay

The result of the previous assay showed a reduction of MPO activity in the mixture with the Gallium arsenide NWs but no insights on the physiochemical mechanism can be deduced. Consequently, the same assay procedure has been refined by the introduction of a preliminary step of centrifugation. Centrifugation allows the separation of particles and biomolecules via spinning of a rotor at a speed of around 13000 Revolution Per Minute (RPM) due to the application of a centrifugal force that affects the sedimentation rate of the different components in a mixture.

Therefore, different components will occupy different regions of the centrifugation tube according to their density, in our system the nanowires are by far denser than MPO, so they will sediment earlier forming a bottom layer called pellet layer while the free protein in solution will remain on top of the pellet layer constituting the supernatant (from the Latin whatever floats on top). The comparison between the activity of the two layers was carried out to assess the eventuality of protein binding to the wires. In fact, in case of protein binding to the wires the enzyme is dragged in the pellet layer together with the wires resulting in an increase of the activity measured for the pellet layer in relation to the activity detected in the supernatant which will be eventually deprived of active enzyme. The microcentrifugation of 100 ul of the previously tested assay solution has been performed with rotational speed set at 13000 RPM for 15 minutes. Subsequently, the isolation of the supernatant from the pellet was effected via pipetting of 90 ul from the centrifuged tube.

The solutions were then tested into the high throughput absorbance reader on a Costar 96 non-binding plate, the instrumental setup requires a minimum volume of 50 µl per well to correctly perform the absorbance reading so the solution was both brought to a volume of 200µl by addition of PBS buffer. Then 3 samples per concentration have been tested 3 times in order to confirm the trend and get reliable statistic. The value of the average endpoint of the absorbance obtained is shown below, while the error bars value is represented by the standard deviation of the measured endpoints in the dataset.

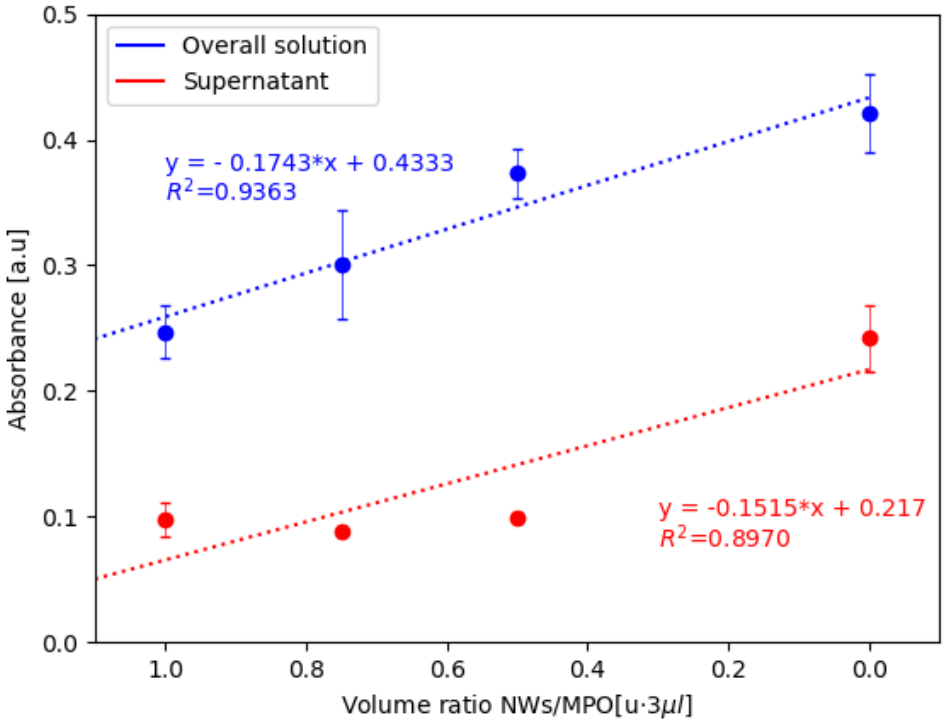

Figure 9 Activity assay after centrifugation and collection of the supernatant. The activity slope is negative due to a change of orientation in the graph axis. Naturally the activity value is absolute value of the slope.

The data confirmed the hypothesis conceived since there is a considerable difference between the activity of the 2 layers with a decrease of the absorbance in the supernatant layer that suggests that MPO is bound to the Gallium Arsenide Nanowires.

Nevertheless, limited information on the physiochemical environment can be deduced by colorimetry since the variation in intensity of the absorbance peak depends mainly on the concentration of chromophore in solution.

In attempt to further investigate possible MPO's structural modifications due to the interaction previously detected, fluorescence measurements were carried out which will be discussed in the following chapter.

References

[1] Robert A. Copeland *Enzymes: A Practical Introduction to Structure, Mechanism, and Data Analysis,*2000, Wiley-VCH, Inc. ISBN: 0-471-22063-9

[2] Johann Heinrich Lambert, *Photometria sive de mensura et gradibus luminis, colorum et umbrae, 1760 Klett*

[3] John L. Monteith and Mike H. Unsworth, *Chapter 4 - Transport of Radiant Energy,* In *Principles of Environmental Physics,* Academic Press, Boston, 2013, Pages 37-48, ISBN 9780123869104, https://doi.org/10.1016/B978-0-12-386910-4.00004-4.

[4] Ingle, J. D. J.; Crouch, S. R. *Spectrochemical Analysis*. (1988) New Jersey: Prentice Hall.

[5] Leah A. Marquez and H. Brian Dunford, *Mechanism of the Oxidation of 3,5,3,5-Tetramethylbenzidine by Myeloperoxidase Determined by Transient- and Steady-State Kinetics*, Biochem. 1997, 36, 9349-9355

[6] David I. Pattison, Michael J. Davies & Clare L. Hawkins (2012) *Reactions and reactivity of myeloperoxidase-derived oxidants: Differential biological effects of hypochlorous and hypothiocyanous acids,* Free Radical Research, 46:8, 975-995, DOI: 10.3109/10715762.2012.667566

[7] M. Wojdyr, *Fityk: a general-purpose peak fitting program,* 2010, J. Appl. Cryst. 43, 1126

[8] Devore, Jay L.,*Probability and Statistics for Engineering and the Sciences (8th ed.).* Boston, MA: *(2011)* ISBN 0-538-73352-7.

Chapter 4: Photophysics

4.1 Fluorescence: lights from chemicals

I can still recall the sensation of safety while I was holding a glowing-in-the-dark dolphin toy when I was a child. Its gleamy light gave me a lot of comfort and I was curious about the origin of that dim glow, so I asked my father who replied, now I know, correctly phosphorescence.

Light-matter interaction whose luminescence and fluorescence are only a partial manifestation, is one of the most relevant topics in physics. It represents the fundamental phenomenon that allows us to know the matter around us. Thus, most of the spectroscopic techniques such as fluorescence spectroscopy rely on a simple paradigm that can be explained as impinging light, interaction, collected modified light. The key role is played by the interaction which modifies the properties of the emitted light according to some property of the substance probed such as chemical composition or physiochemical environment e.g. X-ray Photoelectron Spectroscopy and Fluorescence spectroscopy respectively.

In this chapter, starting from basics principles, the point of focus will be brought on Fluorescence and its application in studying biologically active compounds as MPO.

Fluorescence and Phosphorescence are the characteristic emissions of light following the excitation of specific molecules called fluorophores. Both of these luminescent emissions consist in a relaxation phenomenon i.e. requires an initial activation energy that is provided by the incident light. The radiation excites the fluorophore to a non-equilibrium state with a higher energy to the ground state, this excess in energy is then rebalanced via different phenomenic routes [1].

According to the relaxation pathway which is strongly correlated to the lifetime of the molecular states involved in the deexcitation process the emissive phenomenon is named alternatively fluorescence or phosphoresce. In detail, the fluorescent emission occurs in the order of tenths of nanoseconds (10^{-8} s) with the process of internal conversion happening in a picoseconds time scale (10^{-12}). Phosphorescence, instead, is the product of an ultrafast spin-conversion phenomenon known as intersystem crossing which brings the molecule in a long-lived triplet state whose emission limetime ranges from tenth of millisecond (10^{-5} s) to hours (10^{3} s). The time scale for molecular transition s are in the order of femtoseconds which is order of magnitude faster than the nuclear motion therefore the process of absorption and emission of light are considered vertical transitions in according with the Franck-Condon principle [1].

Alexander Jablonski developed a simple and intuitive scheme for the visualization of the different energetic levels and relaxation pathways. The Jablonski diagram depicted in figure 10 represents the possible vibronic states and transition for a given molecule: the electronic

transition is usually represented as a bold line with a progressive index for the different energetic level e.g. S_0, S_1…… S_n while the broadening given by the vibrational pattern is denoted with a soft line.

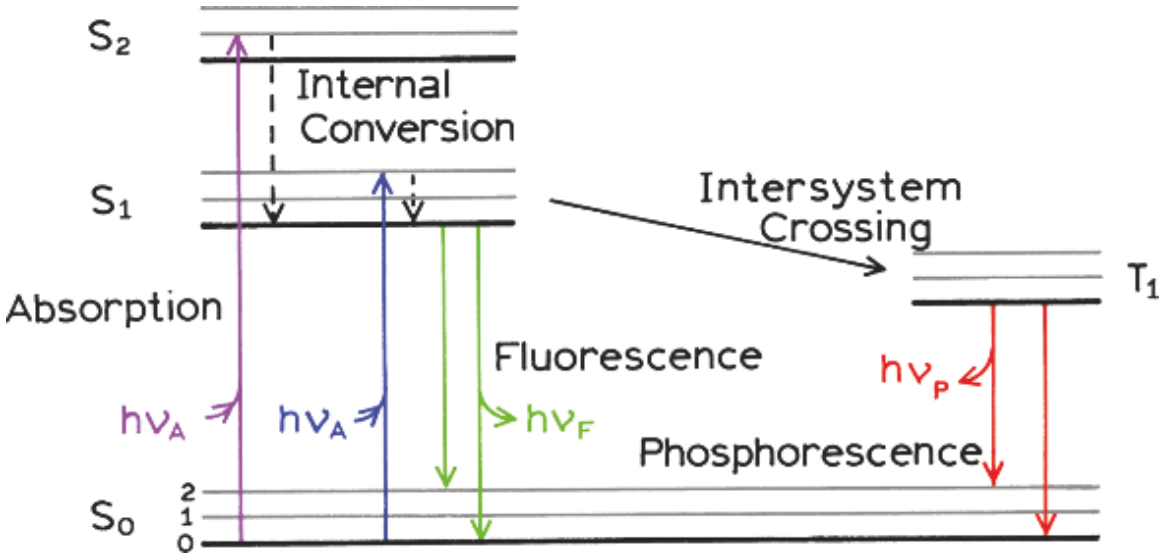

Figure 10 Jablonski Diagram [1]

4.2 Extrinsic probes

Dyes are chemicals with a determined electronic and chemical structure so that the fluorescent state is located at a specific wavelength of interest and the quantity of photons emitted per incident photon i.e. the quantum yield is highest as possible. They are usually implemented to tune the wavelength of emission of the labelled compound. In the case of proteins dyes are usually used to bring the UV emission of biomolecules in the visible range and enhance their detection due to the superior sensitivity of the optical detectors [1].

The point of focus of this section will be brought on the use of a dye compound namely 1,8 anilinonaphthalene (ANS) in the conformational study of proteins. In the results part, ANS fluorescence will be used to investigate MPO's conformational modification when exposed to the Gallium Arsenide nanowires.

1-8 ANS fluorescence behaviour has been object of study since 1965 when L. Stryder investigated the behaviour of the dye and characterizing the utility of using the compound as a probe for testing the presence of hydrophobic area or patches on the surface of proteins. [2].

The mechanism of ANS fluorescent emission can be easily explained towards the Jablonski diagram. In about 1 fs, the absorption of photon at 350 nm shuttles the electrons in a non-equilibrium excited state. Emission of the photon instead takes place from the excited state after an initial relaxation process involving neighbouring solvent molecules, the molecule is in the state S_1. Loss of energy brings the dye to the ground level in a non-equilibrium ground state that is subsequently converted via internal conversion into the equilibrium ground state (S_0) [3].

Even though, since Stryder, ANS has been used as discriminant hydrophobicity of a protein surface patches, more recent studies have put in discussion the assumption that absence of changes in fluorescence corresponds to a higher level of hydrophilicity.

Generally, considering that the main reason for the dye in binding to proteins and poly-amino acids is Coulombic interaction, the event of ANS binding greatly outnumbers the exhibition of intense fluorescence. Therefore, the event of binding is not a sufficient condition for the manifestation of intense fluorescence.

Certainly, hydrophobicity and absence of fluorescence quenching by water molecules remains a prerequisite for the increase of the fluorescence yield but, considering that the lack of variation as a sign of impossibility of binding leads to incorrect deductions [3].

For example, Lysozyme has some hydrophobic superficial patches which bind a maximum of 17 ANS anions in acidic pH but no increase in the yield has been detected. Nevertheless, a number binding sites not accessible to ANS in the native state of the protein only become accessible after denaturation reinforcing ANS role in probing conformational changes [3]. Therefore, extrinsic ANS fluorescence will be used in order to asses MPO's stability range and entity of influence by the Gallium arsenide nanowires.

4.3 Intrinsic amino acids fluorescence

Long chains of amino acids eventually folded i.e. protein do not exhibit particular fluorescent behavior since the possible fluorescent amino acids are only three out of possible 20. These amino acids are phenylalanine tyrosine and tryptophan, which comprise 1% of the mass of all known proteins. They both absorb and emit light in the UV range from 210 to 355 nm, so their fluorescence is invisible to the naked eye [1].

The most extensive studied amino acid with regards to its fluorescent properties is tryptophan (trp) since it possesses the highest yield compared to the other residues see table. Moreover, the most intriguing characteristic of tryptophan emission is the sensitivity to the physiochemical environment. This dependence can be explained analyzing the chromophore generating trp emission i.e. indole. Indole is the conjugation of a benzenic ring with a heterocyclic aromatic pentagon where the nitrogen atom conventionally occupies position 1 see figure 11.

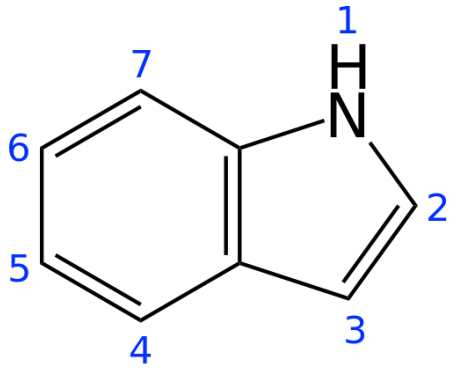

Figure 11 Indole group in Tryptophan residues. reproduced from [4]

During the excitation the electronic distribution varies asymmetrically across the indole rings, therefore any variation in the polarity of the trp residue's surrounding affects the entity and the direction of this induced dipole moment whose relaxation ultimately affect the position and the intensity of the emission peak of the tryptophan residue [5].

A further factor of complication is constituted by the fact that the indole ring of tryptophan possesses two almost isoelectronic fluorescent states namely ^1L_a and ^1L_b. Quantum mechanical simulations in the regime of configuration interaction associate the transitions respectively to HOMO to LUMO excitation for ^1L_a and a linear combination of HOMO - LUMO + 1 and HOMO - 1 to LUMO excitations for ^1L_b transition [5].

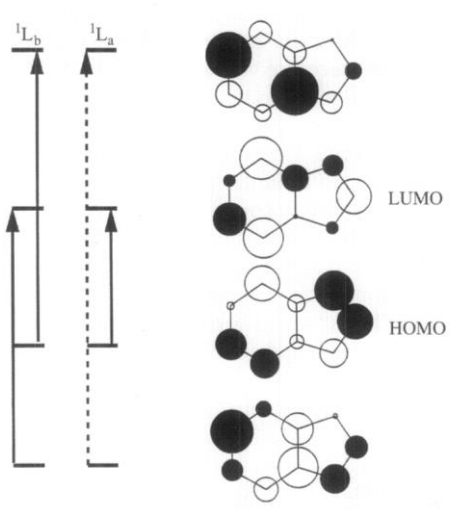

Figure 12 Molecular orbital configuration during $1L_a$ and $1L_b$ transition in indole in vacuum. Calculated ab initio with INDO/S-CI simulation the phase of the wavefunction represented in black and white colour in arbitrary unit. Modified from [5]

For the ^{1}La transition, it can be noticed that the charge distribution is considerably depleted from Nitrogen 1 and Carbon 3 and deposited at Carbons 4, 7, and 9 (there is variation in both the module and the sign of the MO). This process of depletion and deposit causes the dipole moment to increase up to 10 D. On the contrary, for the ^1L_b transition the entity of the polarization is lower, with the dipole generated in the order of the single Debye [5].

Discrimination between the two different fluorescent states is not trivial, because it depends on solvent, experimental conditions and involves quantum mechanical computation methods. Generally, unstructured emission is assigned to the ^1L_a transition since the major role is played by the vibronic broadening due to complexation with solvent molecules while on other hand structured emission is presumed to be generated by the ^1L_b [5].

All these considerations presume that the experiments are conducted tat low temperature (77 to K) therefore at room temperature thermal broadening prevents the identification of the fluorescent state. Nonetheless the sensitivity to the environment character of indole emission is still maintained therefore tryptophan intrinsic fluorescence in protein provides insights on the molecular microenvironment of the different residues [4].

4.4 Tryptophan fluorescence in Proteins

A lot of effort has been put into understanding the behavior of tryptophan fluorescence in proteins in order to correctly clarify the correlation between Stoke-shifted emission and variation of the quantum yield for trp residues. The first quantification of the Stokes shift as a solvatochromic effect fluorescence was provided in 1956 by the Lippert-Mataga equation [1]:

$$|\Delta\bar{\nu}| = \frac{2}{hc}\left(\frac{\varepsilon+1}{2\varepsilon+1} + \frac{n^2-1}{2n^2+1}\right)\Delta\mu^2 \text{ [1]}$$

Where h and c are respectively the Planck's constant and the speed of light in vacuum while ε is the dielectric constant of the solvent and n its index of refraction, while $\Delta\mu$ is the variation in dipole moment between the excited and the ground state. this equation does not take in account the possibility for the fluorophore to be part in hydrogen bond since it will alter the polarizabilty of the microenvironment.

One fist development in the application of Lippert's equation was carried out by Konev's work who proposed the concept of discrete states of tryptophan in protein in attempt to correlate the origin of the spectral shift in different proteins. Konev proposed a two-state model that explained the shifts detected while failed to justify intermediate states [6].

Konev's model was expanded in a 5 discrete states theory by Burstein in 1973 who included results on methyl indole compounds obtained by Hershenberg two year earlier [6]. Hershemberg's findings introduced the possibility of conjugation of the excited residues via hydrogen bonding to solvent molecules or nearby polar residues which leads to the formation of the so called exciplexes. The presence of these intermediates breaks the validity of the Lippert equation so that the stokes shift value can assume also intermediate values between the two previously postulated [6].

Thus, Burstein's model discriminates the different Trp residues based on the relaxation pathway after excitation. The 5 class states are listed in the table below:

Class	Peak maximum in nm (λ_m)	FWHM in nm ($\Delta\lambda$)	Mechanism of relaxation
A	308	n/a, structured spectra	Buried tryptophans in apolar environment incapable of forming exciplexes
S	316	n/a, structured spectra	Buried tryptophans in slightly polar environment that supposedly form exciplexes with stoichiometry 1:1
I	330-322	58-50	Buried tryptophans in polar environment that supposedly form exciplexes with stoichiometry 2:1
II	340-342	53 – 55	Tryptophan exposed to water bound within the proteic structure. Long dipole relaxation times but longer than the lifetime of the excited state. Incomplete red shifting of the emission
III	350-350	59 – 61	Tryptophan exposed to mobile solvent molecules able to complete relax in the excited state

Table 3 Tryptophan spectral classes and mechanism of relaxation in the excited state [5]

This classification expands the parameters that regulates fluorescence emission since it considers both solvatochromic effects (polarizability and refractive index) and the residue's microenvironment in the protein structure (possibility of forming hydrogen bonds). Table 3 exemplifies the spectral features relative to the different classes.

The cardinal step in the evaluation and testing of Burstein's model has been accomplished with the development of an algorithm that allows the decomposition and classification of the different spectral contributes. The algorithm has been tested and via the analysis of more than 160 proteins with a number of tryptophan residues from 1 to 4, in this thesis there is an attempt to expand PFAST computational analysis to a protein with multiple chromophores such as Myeloperoxidase [7].

4.5 Computational structural analysis

In this section, I will proceed to explain the working principle of PFAST´s algorithm as well as its application in the study of MPO-GaAs NWs interaction.

PFAST is a web-based suite of computational tools which base their reliability on the multiple classes model explained in the previous chapter. The first tool is FCAT (Fluorescence Correlation Analysis Tool) that operates a deconvolution of different spectra in spectral components relative to the different classes. The second tool is called SCAT (Structural Correlation Analysis Tool) which performs an *a priori* computation of the different protein residues directly from the Protein Data Bank (PDB) database [7].

4.6 PFAST decomposition analysis

The decomposition of a spectrum in elementary components is considered mathematically a reverse ill-posed problem that consist in the determination of the contributes which summed up reach the maximum level detected from the spectrometer [6]. The solution to this type of problems have low stability towards the variation of the input data i.e. even a low degree of noise can cause a remarkable change in the found results. In order to improve reliability of the FCAT algorithm as well as simplify the computational load, necessary approximations are considered. these constraints though are relative to the physic model of fluorescent emission [6].

- The spectral shape considered is a biparametric log-normal function
- Negligible effect of fluorescence quenching by small molecules other than solvent ones i.e. position and amplitude of tryptophan peaks remain unchanged so that the spectral components in a series of datasets are sum of the elementary contributes.
- The experimental dataset contains a greatly superior number of points compared to the fitting parameters, i.e. the influence of experimental noise is lessened

Given the aforementioned considerations the contribution of the single components to the overall spectrum can be expressed as: [6]

$$F_{i,j} = \sum_{k=1}^{L} I(k,i)\phi(k,j)$$

Where $F_{i,j}$ is th experimental intensity, I(k,i) is the intensity of the k-th component at the i-th concentration, ϕ is the value of the log normal function of the kth component at wavelenght j, j is the wavelength position of maximum, k = 1,...,L is the number of component determined by the position of its spectral maximum.

The log normal function values are retrieved via fitting procedure in according to the criterion of the Root Mean Square (RMS)

The SCAT module instead analyzes the Trp environment in the crystal structure from the datafile in the Protein Databank. Through a complex system of parameters that the SCAT algorithm assigns the different tryptophan to a class taking in account all the possible interaction of the designed residue with the environment. In particular the parameters considered are: packing density of atoms in a radius of 5.5 or 7.5 Å, presence of possible donor-acceptor for Hydrogen bonding, general polarity of neighbouring amino acids and exposure to the solvent via water molecule test [6]. So, the typical set of values relative to a determinate class constitutes the so-called centroid, a model tryptophan that embodies the spectral features for the class. The probability of a real residue to belong to the given class is calculated as a distance from the centroid called Mahalanobis Distance. The Mahalanobis distance is calculated as follows

$$D_m = \sqrt{(\mu_i - x_i)^2 S^{-1} (\mu_i - x_i)^T}$$

Where S is the covariance matrix that weighs the interdependence of the aforementioned variables while μ_i is the average value of the multivariable vector defining the centroid with class i while x_i is the multivariable vector of the tryptophan expressed in the centroid variables [6-7].

The initial six component vector representing all the translational and rotational degrees of freedom for a body in the three-dimensional space is then reduced through a complex mathematical procedure retrievable here in a two-dimensional space of roots which are a linear combination of the degrees of freedom. This mechanism reduces considerably the computational load, so the results are available in few minutes [6]. The SCAT analysis provides a dataset with the list of all the trp residues in the protein with their probability of belonging to a determinate class from A to III weighted by their Mahalanobis distances from the centroid of the class itself. In order to establish a comparison between the SCAT and the FCAT tools, the contributions from different residues were additionally averaged on the basis of intuition to create a "mock spectrum" that takes into account all the contributions to the spectrum by tryptophans belonging to the same class. The mock spectrum is thus composed by the weighted mean of the single contributes with respect to the probability of belonging to a certain class. Provided that, we can define that the statistical weight for a single residue is equal to the probability of belonging to a determinate class

$$W_i = P_{i,k} \; with \; k = A, S, I, II, III$$

With i number of the residues in the sequence and probability P given by the algorithm. Thus the statistical weight for a determined class is the sum of the different contributes of

$$W_k = \sum_{i=1}^{10} W_{i,k}$$

the final intensity is then given by the normalization of the statistical weight with respect to the sum of all possible contributes of the different trp residues.

$$I \propto \frac{W_k}{\sum_A^{III} W_k}$$

There is no reason to furthermore discern the different contributes outside the pertinence to a determinate class i.e. each tryptophan belonging to a certain class is considered identical.

The result is a 4 components spectrum with the relative intensities shown below (fig 13). The total intensity has been normalized to 1000 counts which is the threshold of sensitivity for the Luminesce Spectrometer LS 50 B used to collect the real spectra.

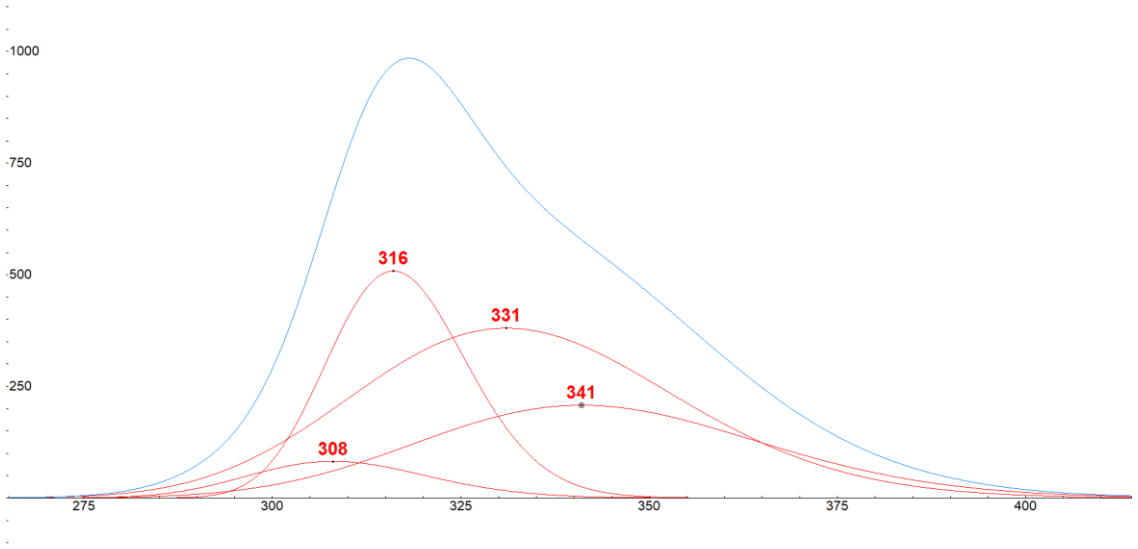

Figure 13 Intrinsic fluorescence spectrum of crystalline MPO. Modelled according to the SCAT algorithm results

Experimental procedure
Different solutions were prepared following the subsequent recipe:

5 µl MPO in phosphate buffer with a concentration 100ug/mL
5/10/15 µl GaAs Nanowires in Ethanol
190/180/175 µl Phosphate buffer (PBS) pH 7.0.

Mix initially the protein and the wires solution then incubate for 15 minutes then dilute with the PBS until reaching 200 µl in an Eppendorf's tube. Pipet 60 µl of sample in Hellma QD 3mm quartz cuvette in the cuvette and record the spectrum. Handle the exhausted solution in nanomaterial waste disposal without dispersion in the environment Repeat 3 times per concentration of NWs after washing of the cuvette. Cuvette washing procedure:

- 3 times Rinsing with MilliQ water
- 10 minutes in cleaning solution Hellanex 2%
- 10 times washing with MilliQ water
- Rinsing once with Ethanol 95%
- Dry with Nitrogen jet at a pressure

The spectra obtained are shown in figure 14

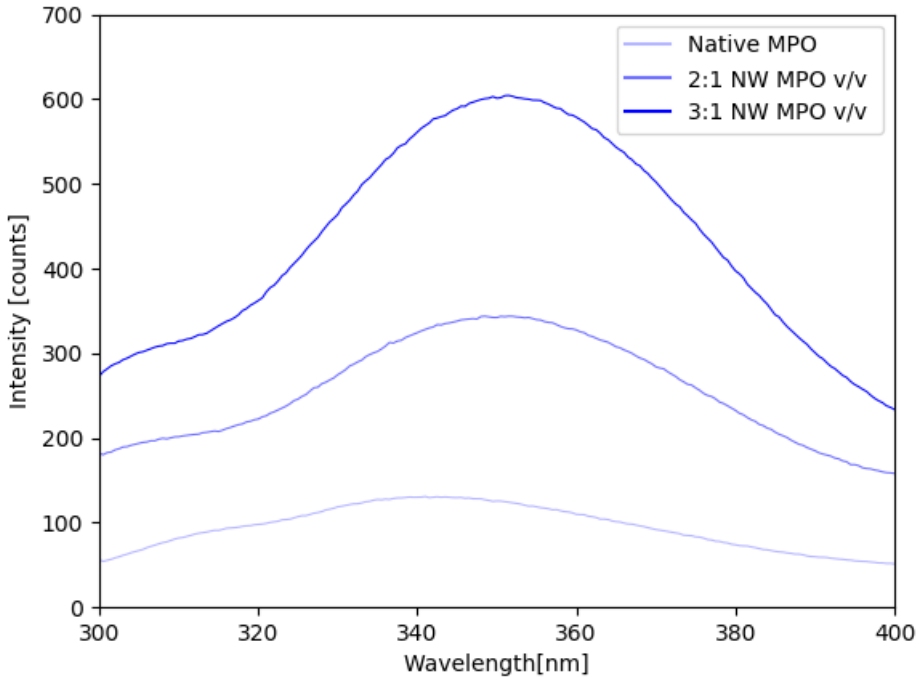

Figure 14 Intrinsic fluorescence spectra of native MPO and MPO bound to Gallium arsenide nanowires

An evident difference can be easily noticed between the calculated spectra and the collected. The major explanation can be retrieved in the different protein configurations assumed between the crystal form and in solution. After introduction of the nanowires in the sample, it is possible to detect a red shift of the most intense fluorescence peak from 349 to 356 nm. As explained in the previous section of the paragraph red shifted emission is an index of major exposure to solvent due to molecular unfolding.

In order to confirm the experimental results, the datasets relative to the spectra have been analysed with the FCAT algorithm. According to the algorithm model, the red shift detected in the peak position highlights the change in the class of one or few tryptophan residues. Due to the large amount of tryptophans in MPO, it is impossible to determine exactly the shift-involved indoles. Nonetheless it can be deduced that, upon binding to the nanowires the contribution to the class III spectral component increase quite sensibly. This suggests that MPO assumes at least a partially unfolded structure when in contact to the nanowires, the here presented trace of unfolding could be a possible explanation for the reduced enzymatic activities shown in the previous chapters of the thesis. The results of the SCAT computation and FCAT analysis are shown in the table below. The value relative to crystalline MPO have been calculated following the approach explained in the previous section of the chapter.

Sample	Number of peaks fitted	Average error of decomposition	λ Max [nm]	Percentage contibution [%]	Class
Crystalline MPO	4	A priori calculation on Crystallline structure 1CXP in Protein Data Bank	N/A	50.2 28.9 20.1 0.8	S I II A
Native MPO	2	3.411	329 341	50.2 49.8	S/I II
MPO NWs 1:2 v/v	2	0.711	307 355	27.6 72.4	A III
MPO NWs 1:3 v/v	2	0.6	309 352	24.3 ± 2 75.7 ± 2	A III

Table 4 MPO Intrinsic tryptophan fluorescence deconvolution

Another important feature revealed by the computational tool is the blue shift of the secondary peak from 329 nm to 306 nm. A possible interpretation could be researched in the dynamics of unfolding that could possibly cause a burying phenomenon for previously exposed residues. Further experiments are required to confirm these hypotheses.

References

[1] Lakowicz, J.R.*Principles of fluorescence spectroscopy*(2011) Principles of Fluorescence Spectroscopy, pp. 1-954. DOI https://doi.org/10.1007/978-0-387-46312-4

[2] Lubert Stryer, *The interaction of a naphthalene dye with apomyoglobin and apohemoglobin: A fluorescent probe of non-polar binding sites*, 1965, Journal of Molecular BiologyVolume 13, Issue 2

[3] Jan Slavík, *Anilinonaphthalene sulfonate as a probe of membrane composition and function*,1982, Biochimica et Biophysica Acta (BBA) - Reviews on Biomembranes, Volume 694, Issue 1,

[4] By Jynto,Own work, CC0,https://commons.wikimedia.org/w/index.php?curid=20495970, Last retreived 18/04/18

[5] Patrik R. Callis, *1La and 1Lb transitions of tryptophan: Applications of theory and experimental observations to fluorescence of proteins*,Methods in Enzymology,1997 Academic Press,Volume 278

[6] Dr. Yana Reshetnyak, http://pfast.phys.uri.edu/background/background.php, 2005, Last retrieved 17/04/18.

[7] Yana K. Reshetnyak, Edward A. Burstein, *Decomposition of Protein Tryptophan Fluorescence Spectra into Log-Normal Components. II. The Statistical Proof of Discreteness of Tryptophan Classes in Proteins*, 2001,Biophysical Journal,Volume 81, Issue 3,Pages 1710-1734,

Chapter 5: Cryo-Electron Microscopy

Sight is the most sensitive and developed human sense. This evolutionary trait has deeply influenced the way our brain processes information. Images usually provoke a stronger reaction with respect to text messages. Naturally, any development that enhanced the human possibility to handle images generated huge impact on the idea and representation of the world. Science as a modern pioneer of progress has always used pictures, drawings and images to sustain or confute various hypotheses. Technical development in collection of images from microscopy sources has greatly morphed the conception and modeling of natural phenomena. For example, optical microscopy has allowed to visualize different tissues and cells within.

In this chapter it will be briefly discussed the fundamental principles of electron microscopy and the evolution that allowed to apply this technique to biological samples. Without the development of cryo-electron microscopy the analysis of a biomolecule in solution would have remained a utopia.

5.1 Electron Microscopy: over Rayleigh´s resolution limit

The optical resolution concept is easy to experience in common life, it is just needed a night promenade close to a street. Eventually, a car or a vehicle with two front lights will come towards the pedestrian. When the vehicle is sufficiently far the eye of the observer will perceive the two light sources as if they were one, they are not resolved, as the vehicle approaches the pedestrian will be able to recognize that the sources are distinct. The resolving power of the human eye can be calculated via the Rayleigh criterion, the Rayleigh criterion considers two source points as resolved then the minimum in intensity of one of the sources coincides with the position of the maximum of the other.

$$\theta = 1.220 \cdot \frac{\lambda}{NA} [1]$$

Considering wavelength in the middle of the visible spectral range e.g 500nm and the numerical aperture of the human pupil as 5 mm immersed in a fluid with refractive index 1.3., the limit of detection of the human eyes results to be 3 microns [1]. Nonetheless, due to aberration in focusing of the crystalline lenses the minimum distance for a clear perception is 25 cm that correspond at a resolution of 75 microns according to the Rayleigh criterion given an angular resolution of 3 10^{-4} rad [1]. Conceptually, lenses in optical microscope bring to the resolution limit the dimension of smaller objects. The best magnitude enhancement attainable via optical microscopy is 250x that is sufficient to visualize bacteria or organelles in cells, but superior magnification is required to image the fundamental building blocks of nature i.e. DNA and atoms.

Objects in the nanoworld require a magnification factor from 40 000x to 400 000x which is beyond the capabilities of optical microscopy. Fortunately, the Rayleigh criterion allows also to adjust the wavelength of the incident radiation to improve the minimum resolvable distance.

The basic concept for a cardinal revolution in microscopy was elaborated in the early 20th century when Louis De Broglie enunciated the principle of wave particle duality.

$$p = \frac{h}{\lambda}$$

Where p is the momentum of a particle, in our case electrons, and h is the Planck's constant, λ is the wavelength of the particle's matte wave. Therefore, even electrons can be used as a source of "light" for imaging purposes. The technical development required to focus and detect electrons i.e. electromagnetic lenses and detectors were reached in 1932 when David Ruska operated for the first time an electron microscope managing to successfully record high resolution image of cotton fibers [2].

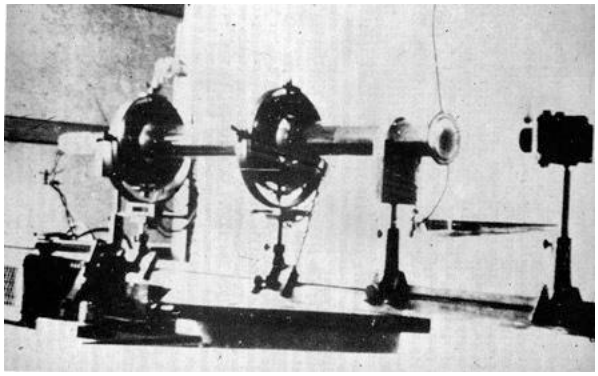

Figure 15 Ruska's first electron microscope [2]

As shown in fig 14 Ruska's setup was aligned horizontally on the working plane but this caused troublesome difficulties of alignment for the electromagnetic lenses. Thus, already in 1934, the first commercial electron microscope assumed a vertical arrangement [2]. The electron production in the early stage of development was ensured by a gas discharge tube. The voltage spikes connected to the gas discharge were a substantial source of damage for the samples, so they were almost immediately substituted with tungsten filaments, which produce electrons by thermoionic effect. At present electrons for microscopy are generated via field emission guns where a sufficiently sharp tip of materials like LaB_6 or tungsten is invested by a strong electrical field so that electrons on the top of the conduction band can be emitted by the tip. Field emission guns require Ultra High Vacuum (10^{-8} Pa) conditions to operate, in this regime the electrons produced can travel distances of kilometres before being stopped.[1]

The requirements of UHV conditions and intense electronic radiation, were soon declared unadapt for the analysis of biological samples by Marton in 1934 [3]. The cardinal revolution in microscopy seemed only to involve inorganic matter. Bio-related molecular sciences had to wait more than sixty years to embrace the advantages of electron microscopy. Thanks to the work of Jacques Dubochet, Joachim Frank and Richard Henderson, who were awarded the Nobel Prize in Chemistry in 2017, electron microscopy is nowadays applicable also to

biomolecular material. Their development of cryo-electron microscopy has enabled us to capture biomolecules directly in solution, in their native state [4]. The mechanism and the principles of Cryogenic Electron Microscopy will be discussed in the following section.

5.2 Biomolecules: problematic specimens and solutions

Why biological sample analysis was problematic for electron microscopy?

First reason, the sample chamber needs to be maintained in UHV conditions o that the mean free path of electrons reaches considerable length before being detected. For example the mean the Mean Free Path at atmospheric pressure is which while in UHV the distance . Moreover, the lack of external pressure forces the water naturally embedded in biological samples to evaporate increasing the susceptibility to radiation damage [1].

One of the principal phenomena involving specimens under electron bombardment as in a microscope is radiolysis which consists in the cleavage or rearrangement of chemical bonds caused by energy transfer from inelastic scattered electrons, to valence electrons in the material [1]. The most intuitive solution is to reduce the intensity of the electron beam so that the sample will be invested by lower amount of radiation. The drawback is the dramatic reduction of the contrast between background and specimens which for already low-contrast targets like biomolecule enormously limit the resolution achievable [1]. Radiolytic damage, though, is greatly dependent on thermal motion, so that it is three to ten-fold lessened at a temperature around 100 K [1].

The natural choice to prevent dehydration and radiolysis in biomolecular samples is maintain them in aqueous solution and freeze them at cryogenic temperature. Crystalline ice though diffracts electrons due to the reticular arrangement of the atoms, therefore prevents any possible visualization of cause inhomogeneous electronic absorption the background would unevenly change intensity. In 1981, Debouchet managed to create vitrified water by abruptly cooling water droplets at liquid ethane temperature. (190°C). Vitrified ice exhibited the desired properties of molecular shielding and homogeneous electronic absorption. The era of cryo-electron microscopy has begun [4-5].

At present Cryo-EM has reached atomic resolution for large agglomerates and big proteins up to 100kDa becoming the most valuable source of information in biomolecular dynamics [4]. Cryo EM experiments have been carried out in order to reinforce the conclusions drawn after the spectroscopic measurements and they will be discussed in the subsequent section of this chapter.

5.3 Cryo-Transmission Electron Microscopy: MPO and Gallium Arsenide Nanowires

The enzymatic assays and fluorescence spectroscopy measurement suggest the presence of an interaction between the peroxidase enzyme and the wires. In attempt to find confirmation of the conclusions deducted before, Cryo Transmission Electron Microscopy (CTEM) measurements have been performed using the JEM-2200FS microscope present at nCHREM.

The experimental protocol for the preparation of the sample is shown below.

1. Remove ethanol supernatant from NWs by putting an open tube on the heat block at 60°C and wait until no liquid is visible, resuspend in 50 µL 10 mM phosphate, pH 7.4.

2. Take 15 µL of NW sample, add to 15 µL MPO in 10 mM phosphate, incubate for 30 minutes with resuspension of sample every 10 minutes.

3. Centrifuge at 3000 RPM for 2 minutes, remove supernatant and resuspend in 75 µL phosphate buffer

4. Take 25 µL in a labelled tube, sample #1 (MPONW) with only NWs and MPO.

5. Add the remaining 50 µL sample to a tube of NHS activated gold, 5 nm.

6. Incubate for 15 minutes, resuspend every 5 minutes.

7. Centrifuge at 3000 RPM for 2 minutes, remove supernatant, resuspend in 50 µL 10 mM phosphate. Repeat.

8. Label sample #2 (MPONWAU).

Once prepared 4 ul of the sample were disposed on a glow-discharged lacey C copper TEM grid. The grid is composed by 300 meshes of variable dimension from 60 to 90 micrometers, the support and then plunged frozen in liquid ethane at -176 °C after a blotting time of 0.8 seconds in order to remove liquid in excess. The microscope JEM-2200FS was operated at 200 keV in low dose mode to preserve the integrity of the sample. Images at different magnitudes were collected with the help of electromagnetic slits in order to enhance contrast.

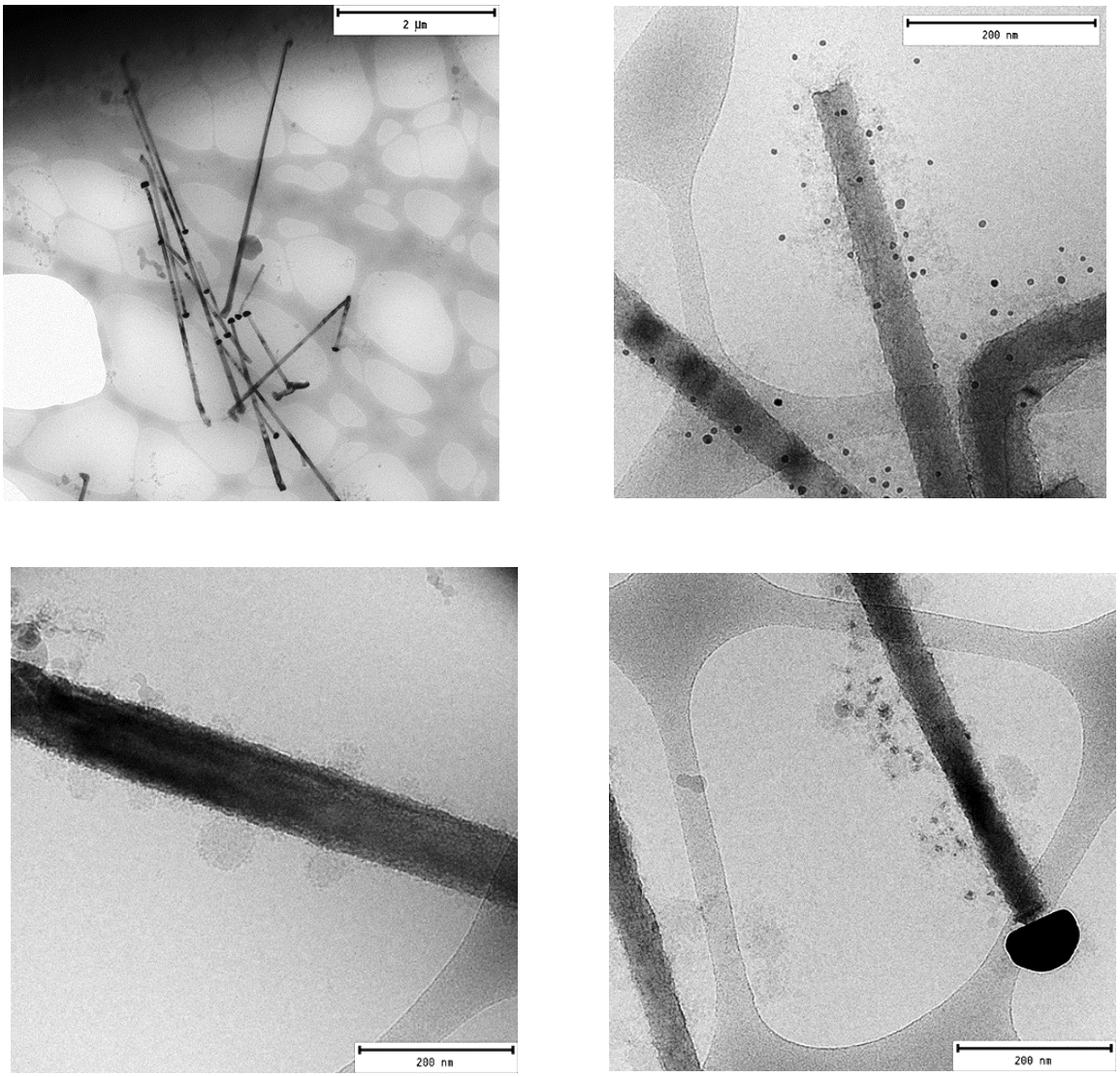

Figure 16 Cryo-EM images of MPO on GaAs Nanowires: Top-left: low magnification image of aggregate of wires. Top-Right: bottom end of nanowire clotted with enzyme and gold particles. Bottom High magnification images of MPO clusters adsorbed on wires

The low magnitude pictures show a strong tendency of aggregation of the nanowires. The protein aggregate is not quite visible at this magnitude since not enough contrast is provided between the wires and the carbon mesh that sustains the sample. Increasing the magnification to 20 000x it is possible to detect the protein surrounding the wires in fact the intensity of the beam is slightly attenuated around the edges of the wires. Since the contrast in a transmission electron microscopy is given by the difference in electronic absorption coefficient, biomolecules which usually have remarkably inferior electronic absorption will appear brighter than metal or semiconductor. The definitive confirmation that the protein lies in the surrounding area of the wires is evidenced in the gold labeled sample where it can be noticed that the gold particles are clustered in the adjacent zone.

In high magnitude image it is possible to notice the lack of a pattern in the disposition of the gold particles indicating that the enzyme assumes different configurations at the interface with the wires. Nonetheless, a definitive statement cannot be done due to the fact that the image is a projection of the

sample onto the detector. Only a series of tomograms can actually determine the exact position and eventual presence of a pattern in the Au-particles disposition that would reflect a particular attachment conformation for MPO.

On the other hand, in the specimen where no gold particles have been attached to MPO the protein seems to assume a globular conformation with variety in the diameters of the structure. In general, the dimension of this globules ranges from 25 to 50 nm. By simple comparison with the diameter of the protein that is approximately it is possible to deduce that multiple enzyme molecules are the constituent of this molten globule structure.

Another interesting feature shown by the collected images is that the diameter of the wires does not correspond to the diameter of the original catalytic gold particle. This is index of a possible corrosion phenomenon happening at the interface between the catalyst and the initial section of the wire. The causes of this degradation of the material are unknown, a possible explanation could be retrieved in a chemical corrosion from the ethanol solvent used in the storage procedure, but further experiments are needed to confirm. From a nanosafety perspective, Gallium Arsenide NWs' instability is a reason of concern since release of arsine ions constitutes a serious risk for human health.

References

[1] R. Egerton, *Physical Principles of Electron Microscopy: An Introduction to TEM, SEM, and AEM*,2016, Springer International Publishing Switzerland https://doi.org/10.1007/978-3-319-39877-8

[2] Ruska, E., *Nobel Lectures, Physics 1981-1990,* Tore Frängsmyr and Gösta Ekspong, Eds. (1993) World Scientific Publishing, Singapore

[3] Marton, L. (1934) *Electron microscopy of biological objects*. Nature 133, 911-911

[4] https://www.nobelprize.org/nobel_prizes/chemistry/laureates/2017/advanced-Chemistryprize2017.pdf last retreived 18/04/18

[5] *Dubochet, J., Adrian, M., Chang, J.-J., Homo, J.-C., Lepault, J., McDowall, A. W., and Schultz, P. (1988) Cryo-electron microscopy of vitrified specimens. Q. Rev. Biophys. 21, 129-228*

Conclusions

The goal of this thesis project was to investigate a possible interaction between novel nanomaterials and an active protein present in the immune system in attempt to assess eventual anomalous responses. The experimental results suggest that an influence is present i.e. reduction of enzymatic activity as well testified by the absorbance assays. Myeloperoxidase's action is strictly related to bacterial killing processes, so the downregulation detected here could be a symptom of an inhibition of the immune response.

Successive tests via fluorescence spectroscopy gave further insights on a possible explanation for the conclusion drawn after the absorbance assays which can be justified as an unfolding event of MPO when bound to the wires. Estimating thoroughly the entity of this interaction could provide even more detailed information about possible effects of nanomaterials. That could be done via nearly-atomic resolution cryo-electron tomography that still has not been applied to MPO yet, while pioneering tomographic models are present for the nanowires.

Generalizing to a more holistic perspective the results exposed in this study are only an embryonal step in the establishment of the toxicological profile of nanowires but nonetheless, they provide insights on the determination of molecular bio-nano interaction. These insights can be interpreted as conceptual building blocks for successive experiments involving other materials and/or other bioactive molecules. Nevertheless, a non-negligible reinforcement of the relevance of the conclusions drawn in the project is embodied by the fact that the materials involved are reasonable candidate to play a role in an eventual contact between nanowires and human body. Aerotaxy-produced Gallium Arsenide nanowires have reached now complete industrialization and implementation in solar cells devices while Myeloperoxidase's primarily relevance in bacterial killing is well known and confirmed throughout the literature, so it constitutes a good candidate to fulfil the scope of the project.

What future will reserve us? Yet to be known, but one thing is certain. Nanotechnology is already impacting the world, nanoobjects are increasingly being part of it. Knowledge about the nanoworld and its interaction with the bioworld is our only way to achieve considerable safety in handling of this new outstanding materials.